University of Glasgow

DEPARTMENT OF

AEROSPACE ENGINEERING

The Estimation Of Helicopter Pilot Workload Using Inverse Simulation

Garry R. Leacock*

Dr. Douglas G. Thomson**

Internal Report No. 9624 September 1996

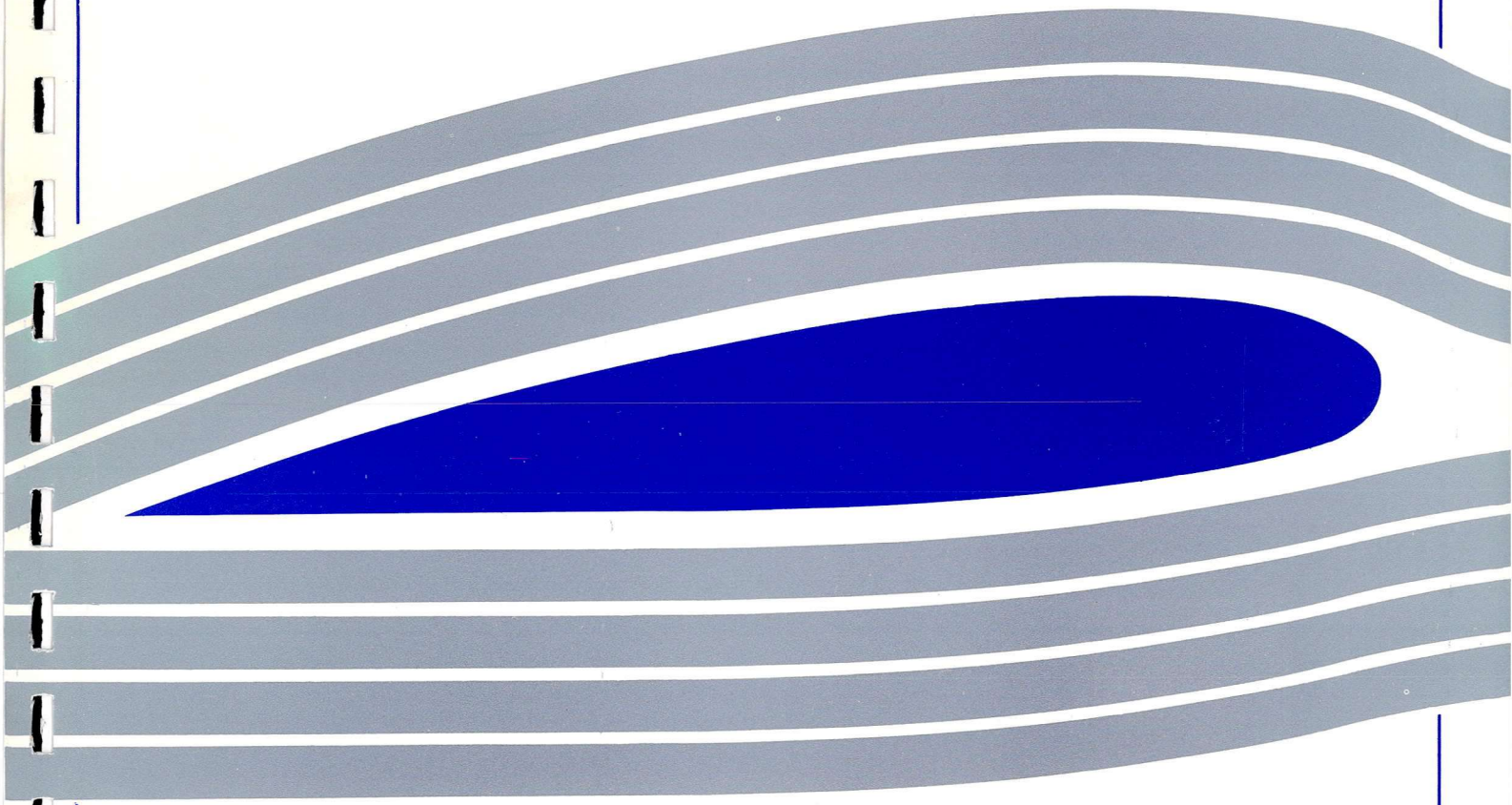

The Estimation Of Helicopter Pilot Workload Using Inverse Simulation

Garry R. Leacock*
Dr. Douglas G. Thomson**

Internal Report No. 9624 September 1996

*Postgraduate Research Assistant
**Lecturer in Flight Dynamics

Department of Aerospace Engineering
University of Glasgow
Glasgow
G12 8QQ
U.K.

Abstract

In the first instance this report describes the means by which inverse simulation can be used as a pilot workload estimation tool. An alternative approach to defining the mathematical model of the ADS-33 Rapid Side-step Mission Task Element (MTE) is presented and is used to drive various inverse simulation runs. Studies are conducted into three varying aggression side-step MTEs and the comparison of two dissimilar helicopter configurations based on the Westland Lynx, simulated using the same side-step. It is shown how the resulting time-histories and quickness charts can be utilised in pilot workload and handling qualities estimation. A third quickness parameter associated with the lateral cyclic stick displacements required to fly the side-step MTEs is introduced and is shown to be capable of discriminating between the pilot workload required for each side-step and vehicle configuration. The latter study in the report presents the preliminary findings on the effects of workload by firstly, introducing a Stability and Control Augmentation System and secondly investigating the effects of altering the value of the lateral cyclic actuator time constant.

Nomenclature

Q_{ϕ} roll quickness parameter

$Q_{\theta 1c}$ lateral cyclic pitch quickness parameter

$Q_{\eta 1c}$ lateral cyclic stick displacement quickness parameter

t_a time to reach maximum acceleration in Rapid Side-step Mission Task Element

t_d time to reach maximum deceleration in Rapid Side-step Mission Task Element

t_m time take to complete entire side-step manoeuvre

V_{max} maximum lateral airspeed attained during side-step

$\dot{V}_{max}$ maximum lateral acceleration attained during side-step

$\dot{V}_{min}$ maximum lateral deceleration attained during side-step

p roll-rate of helicopter

p_{pk} maximum roll-rate of helicopter

ϕ bank angle of helicopter

$\Delta\phi_{min}$ change in roll angle corresponding to time taken for maximum roll-rate

θ_{1c} lateral cyclic pitch

η_{1c} lateral cyclic stick displacement

$I\theta_{1c}$ time integral of lateral cyclic pitch

$I\eta_{1c}$ time integral of lateral cyclic stick displacement

θ_{1cpk} maximum lateral cyclic pitch displacement

$\Delta I\theta_{1c}$ change in pitch integral corresponding to time taken to reach maximum lateral cyclic pitch displacement

η_{1cpk} maximum lateral cyclic stick displacement

$\Delta I\eta_{1c}$ change in stick integral corresponding to time taken to reach maximum lateral cyclic stick displacement

1. Introduction

Good handling qualities play a large role in ensuring the safe and successful execution of a mission by the pilot of any aircraft. The particular ability of the helicopter to fly nap-of-the-earth manoeuvres by its nature demands that the handling qualities be exceptional as insufficient performance can lead to mission failure due to intolerable levels of workload being placed upon the pilot. The assessment of helicopter handling qualities is accomplished by monitoring task performance and flying characteristics, whilst performing a standard manoeuvre or Mission Task Element (MTE). There are a wide variety of MTEs that can be utilised in the appraisal of handling qualities, the fundamental requirement being that the MTE must be accomplished with Level 1, (Cooper-Harper rating of 3 or better) flying qualities throughout the operational flight envelope (OFE) [1].

The Cooper-Harper scale, Figure 1, is generally regarded to be the most developed and universally accepted method of evaluating handling qualities ratings. The scale ranges from 1 to 10 and is split into 3 basic 'levels':

- Level 1 - satisfactory without improvement, minimal workload
- Level 2 - desired performance requires moderate compensation OR deficiencies warrant improvement, adequate performance requires considerable to extensive compensation
- Level 3 - deficiencies require improvement, adequate performance unattainable with tolerable pilot workload

A helicopter that achieves a rating of Level 1 is seen as attaining the minimum required standard, which is measured in terms of task performance and pilot workload. Level 2 is acceptable in emergency and failed situations only, while Level 3 is unacceptable and describes an aircraft with major deficiencies.

The most recent specification for flying and ground handling qualities of rotorcraft, is the Aeronautical Design Standard ADS-33, Handling Qualities For Military Rotorcraft document [2] and it assures that no limitations on flight safety or mission performance will result from deficiencies in flying qualities. ADS-33 specifies the requirement of two methods to establish a Handling Qualities Rating (HQR) for any particular helicopter. The first employs the 'quickness' parameter as an objective means of quantifying response properties of the helicopter. This ensures that the aircraft is capable of achieving required attitude changes within a sufficient time scale. The quickness parameter is defined as the peak rate of change to change in attitude and in the roll axis for example, can be calculated from:

$$\text{Roll quickness } (Q_\phi) = \frac{p_{pk}}{\Delta\phi_{min}} \qquad (1)$$

where p_{pk} is the peak roll rate and $\Delta\phi_{min}$ is the corresponding change in roll angle, Figure 2.

Secondly and subjectively, the HQR is captured through the impression of workload from pilots who fly Mission Task Elements. Since this technique is prone to variability and bias, several pilots are required to fly the manoeuvre and the rating is accepted only if the spread of the pilots' ratings is not greater than 2 points on the Cooper-Harper scale.

ADS-33 specifies that simulation should be used as part of a handling qualities assessment programme at various stages throughout the design and flight testing of new aircraft. This involves calculating the response of the aircraft to a particular sequence of control inputs and is a well known practice. Inverse simulation, on the other hand, is essentially the opposite of conventional simulation, as it calculates the control time-histories required to produce a predetermined output. It is potentially an excellent tool for evaluating helicopter handling qualities in manoeuvring flight, as the information collected from an inverse simulation run can be as extensive as data obtained from real flight trials. However, the results obtained from inverse simulations can only be used to determine handling qualities if the

mathematical model employed is of suitable quality and robust enough to adequately represent the flight conditions encountered by the real aircraft. Moreover, the MTE being simulated, and the actual flight trials MTE, must possess a high level of congruity, in order that the resulting output data is of sufficient accuracy to enable further calculations and ultimately handling qualities estimation.

It is the aim of this report to firstly rationalise existing work at Glasgow University on handling qualities estimation using the original definition of the side-step MTE (Section 2.1) and introduce an alternative definition of the manoeuvre (Section 2.2). A number of studies were performed using the alternative definition side-step to drive the helicopter inverse simulation package, Helinv [3], the results of which will be presented in later sections of this report. The second main objective is to present preliminary findings on the effects of:

a) introducing a Stability and Control Augmentation System (SCAS), and

b) altering the time constant on the lateral cyclic actuator (τ_{C2}).

2. Side-step Manoeuvre Definitions

The side-step is a linear repositioning manoeuvre, Figure 3, which initiates and terminates in a trimmed hover state, translating over a calculated linear distance in between. It is assumed that the helicopter's body y-axis is parallel to the earth y-axis, and that no acceleration occurs along either the x or z axes. It is further assumed the manoeuvre is physically symmetrical about the mid point. Inverse simulation of a side-step, or in fact any manoeuvre, is based on the creation of a mathematical description or model of the manoeuvre and at present Helinv is capable of generating results based on either one of two possible side-step definitions as discussed below.

2.1 Mathematical Representation of the Side-step Manoeuvre Using a Global Polynomial Function

One element of work previously carried out at Glasgow University was the development of a library of basic linear repositioning and turning flight manoeuvres [4], which were further developed to encompass the more rigorous demands of MTEs specified by ADS-33. The approach taken was to fit simple polynomial functions to the known profiles of primary manoeuvre parameters, which, in the case of the side-step are; aircraft position, velocity, and acceleration. The side-step manoeuvre is one of the more basic types found in helicopter flight, and can be split into simple constituent parts, onto which specific boundary conditions can be superimposed. Since the helicopter starts and finishes the manoeuvre in a trimmed hover state, implying zero velocity and acceleration at these points, and assigning a further boundary condition stipulating that the maximum velocity reached is exactly half way through the manoeuvre, a sixth order polynomial can be derived from the seven boundary conditions imposed, to yield the velocity profile:

$$V(t) = \left[-64\left(\frac{t}{t_m}\right)^6 + 192\left(\frac{t}{t_m}\right)^5 - 192\left(\frac{t}{t_m}\right)^4 + 64\left(\frac{t}{t_m}\right)^3 \right] V_{max} \qquad (2)$$

where t_m is the time taken to complete the entire manoeuvre. Figure 4a is a graphical representation of this velocity profile and illustrates the smooth nature of the global approximation. It was found that this approximation of the side-step compared favourably with flight test data [5], but because of the smoothness of the profile proved to be insufficiently aggressive to represent a side-step MTE as described by ADS-33. Further analysis in the form of quickness parameter calculations confirmed this line of thinking, and it was clear that additional developments to the side-step model were required in order to capture the aggressive nature of a Rapid Side-step MTE.

2.2 Mathematical Representation of the Side-step Manoeuvre Using a Piecewise Polynomial Function

ADS-33 documents the key elements of the Rapid Side-step MTE as follows:

"Starting from a stabilised hover, ... initiate a rapid and aggressive lateral translation at approximately constant heading up to a speed of between 30 and 45 knots. Maintain 30 to 45 knots for approximately 5 seconds, followed by an aggressive lateral deceleration to hover, ..."

Additional desired performance during manoeuvre

- Maintain the cockpit station within ± 3.3m of the ground reference line
- Maintain altitude within ± 3m
- Maintain heading within ± 10 degrees
- Attain maximum achievable lateral acceleration within 1.5 seconds of initiating the manoeuvre
- Attain maximum achievable deceleration within 3.0 seconds of initiating the deceleration phase
- Stabilise within 1.5 seconds of achieving hover. Heading tolerance is ± 2 degrees

Cleary this is a much more aggressive approach, and that the polynomial described by equation (2) would not be satisfactory in achieving all of the requirements. It is possible to identify seven separate and distinct sections in the above description, and since they are mainly concerned with the acceleration of the vehicle it was decided that the new profile to define the manoeuvre would also be in terms of the vehicle's acceleration. The approach taken was to consider the manoeuvre acceleration profile as being a sequence of individual segments where each segment is representative of the primary acceleration stipulations. The seven sections of the acceleration profile consist of:

1. A rapid increase in lateral acceleration from trimmed hover to a maximum value $\dot{V}_{max}$ after a time t_a seconds

2. A constant acceleration section to allow the flight speed to built up to some maximum value V_{max}, between 30 and 45 knots
3. Lateral acceleration decreased rapidly to zero, after desired flight speed has been attained
4. Zero acceleration held for five seconds, to produce a constant velocity phase
5. A further rapid decrease in lateral acceleration to reach maximum lateral deceleration $\dot{V}_{min}$ after a time t_d seconds
6. A constant deceleration phase to allow flight speed to be reduced towards zero
7. Rapid decrease in deceleration to bring the helicopter to trimmed hover after a full manoeuvre time of t_m seconds

Figure 4b shows these seven sections on an acceleration profile, with the user inputs being t_a, t_d, $\dot{V}_{max}$, $\dot{V}_{min}$ and V_{max}. In order to ensure that the performance limits are met, the values of t_a and t_d are set such that $t_a \leq 1.5$ seconds and $t_d \leq 3.0$ seconds. By specifying an increased number of boundary conditions at each transient stage (phases 1, 3, 5 and 7) in the manoeuvre, the derivation of third, fifth and seventh order polynomial functions was possible, which had the corresponding effect of increasing manoeuvre severity [6] , Figure 5. The effect of higher order polynomial functions is that the initial acceleration occurs more smoothly, but the peak rate of change of acceleration will be greater as the order of the function is increased.

3. The Roll Quickness Parameter (Q_ϕ)

The roll axis is the primary axis used in the rapid side-step MTE and since inverse simulation calculates the time-histories of roll rate p and roll angle ϕ, it is a simple task to calculate the roll or attitude quickness parameter chart, as described by ADS-33C section 3.3, giving an indication to the level of flying quality attained.

In this section of the report, roll quickness comparisons will be made between:

a. three Side-step manoeuvres of varying severity using the same helicopter configuration based on the Westland Lynx battlefield/utility helicopter and,
b. two dissimilar helicopter configurations based on the Westland Lynx, simulated using the same rapid side-step MTE.

3.1 Comparison of Roll Quickness for Varying Aggression Rapid Side-step MTEs

The side-steps are all performed with an initial roll to the right and the severity is increased or decreased by correspondingly adjusting the 'time to maximum acceleration, t_a' and the 'time to maximum deceleration, t_d'. A summary of the parameters imposed on the three side-steps is presented in the table below.

Side-step	V_{max} (kts)	t_a (s)	t_d (s)	$\dot{V}_{max}$, $\dot{V}_{min}$ (m/s^2)
1	35	1.50	1.50	4.000
2	35	1.30	1.30	4.625
3	35	1.10	1.10	5.250

Table 1 Parameters for side-step MTEs, least (1) to most aggressive (3)

The roll-rate and roll angle time histories for the three side-steps are presented in Figures 6a through c. It can be seen that the manoeuvre comprises four distinct pulses; first there is the initial roll into the manoeuvre followed by a roll to an almost horizontal attitude, after which the helicopter will traverse at a constant velocity for five seconds. The third pulse is in the opposite direction to the initial pulse in order to tilt the rotor into a position to decelerate the helicopter and this is succeeded by a final pulse which rolls the helicopter back to the trimmed hover position.

The roll quickness chart corresponding to the time-histories presented in Figures 6a through c is shown in Figure 7 and it can be seen that the values lie mainly in the Level 1 region, which is in keeping with other similar experiments carried out at Glasgow University [6]. Since the time taken to reach maximum acceleration was the same as the time taken to attain the maximum deceleration, it was not unexpected that the pulses of acceleration should produce quickness values similar to the deceleration pulses, as shown.

3.2 Comparison of Roll Quickness For Two Lynx Configurations

Previously, it has been shown that the quickness values obtained from pilot inputs during a rapid side-step MTE increase with the severity of the manoeuvre, using the same helicopter. This section of the report examines the results obtained when using two dissimilar helicopter configurations, again based on the Westland Lynx. The individual discrepancies between each vehicle are summarised in Table 2, the major differences being overall mass and rotor stiffness.

Parameter	Lynx-1	Lynx-2
1: Mass (kg)	3500.00	4250.00
2: Blade chord (m)	0.391	0.300
3: C. G. position from reference (m)	0.00	-0.10
4: Equivalent stiffness for centre-spring blade flapping model (Nm/rad)	166352.00	50000.00
5: Height of main rotor above CG (m)	1.271	0.960

Table 2 Summary of Lynx configuration discrepancies

The two inverse simulation runs were conducted using the second or medium aggression side-step MTE to drive Helinv; the roll-rate and attitude time-histories are plotted in Figures 8a and b. On observing the roll quickness chart for the two configurations, Figure 9, the initial surprising result is that both helicopters produce very similar quickness values. However, this result is characteristic of other similar inverse simulations conducted at Glasgow University, and it is generally accepted that for various helicopter configurations the quickness values obtained will be of a comparable nature, due to the fact that the roll quickness and attitude are dependant on the manoeuvre profile itself; and since both simulations were executed using the same side-step, it follows that the resulting quickness parameters will also be comparable.

Since the roll quickness chart is largely incapable of discriminating between different helicopter configurations, it is of little use as a tool for assessing workload. It can however differentiate between different helicopter performance limits, by imposing a maximum value whenever the helicopter has reached its' control limits. In the above example, as the severity of the side-step is increased, it is probable that Lynx-2 will reach the maximum available lateral cyclic before Lynx-1, implying that Lynx-1 is a more capable aircraft, in that it has a higher spare performance capacity. To properly assess the pilot workload of a helicopter, it is necessary to introduce a second quickness parameter, the Lateral Cyclic Pitch Quickness Parameter ($Q_{\theta 1c}$), which is discussed below in more detail.

4. The Lateral Cyclic Pitch Quickness Parameter ($Q_{\theta 1c}$)

Sometimes referred to as control quickness, the lateral cyclic pitch quickness, when plotted on a chart, produces results that can be used to objectively assess helicopter pilot workload. It is calculated in exactly the same manner as the roll quickness parameter, and is given mathematically as:

$$\text{Lateral cyclic pitch quickness } (Q_{\theta 1c}) = \frac{\theta_{1cpk}}{\Delta I\theta_{1c}} \qquad (3)$$

where θ_{1cpk} is the peak lateral cyclic control displacement and $\Delta I\theta_{1c}$ is the subsequent change in the integral of the lateral cyclic control.

It is worth pointing out at this stage that the equation analogous to roll quickness is given by $\dot{\theta}_{1cpk} / \Delta\theta_{1c}$, and not as given in equation (3). However, experimentation has shown that the resulting quickness charts produced little data that could be utilised in handling qualities evaluation. Instead it was found that the pulses of lateral cyclic observed on the time-histories were similar to the pulses of roll-rate, suggesting that the integral of lateral cyclic pitch, Θ_{1c} would be a more appropriate denominator in the equation. Indeed, this was found to be the case, and as we shall see, the resulting quickness charts plotted using equation (3), have yielded information beneficial to handling qualities studies.

4.1 Comparison of Lateral Cyclic Pitch Quickness for Varying Aggression Rapid Side-step MTEs

The lateral cyclic pitch (θ_{1c}) time-histories for all three rapid side-step MTEs, Table 2, were obtained from the inverse simulation runs conducted in section 3.1. With the aid of the general plotting sub-routine Genplot, (an integral part of the Helinv package), the time-histories for θ_{1c} and its' integral Θ_{1c} were obtained and are presented in Figures 10a through c.

On plotting the subsequent quickness chart, Figure 11, it was again possible to identify the main pulses of acceleration and deceleration in the manoeuvre, and as part of the assessment

of handling qualities, the chart is annotated with hyperbolic lines representing 50% and 100% of the maximum lateral cyclic control limit. It can be seen that the control pulses in the more aggressive side-step approach the 100% boundary more closely than those in the less aggressive manoeuvre, the difference between them representing the additional pilot workload required to conform to the confines of the MTE model. The third rapid side-step is shown to be the most aggressive and it is here that workload is highest, as the helicopter is pushed to the limits of its' manoeuvrability.

4.2 Comparison of Lateral Cyclic Pitch Quickness For Two Lynx Configurations

The lateral cyclic pitch quickness chart presented in Figure 13 was produced using the time-histories in Figure 12. It can be seen that it is an excellent tool for discriminating between the two helicopters, as it identifies Lynx-2 as being an inferior helicopter since a pilot would be required to make larger control inputs to perform the same manoeuvre. This is represented on the chart simply by the fact that the quickness value points for Lynx-2 approach the 100% contour more closely than those of Lynx-1, suggesting that a higher percentage of the maximum lateral cyclic control is being used.

It has been illustrated that inverse simulation of a side-step manoeuvre, coupled with the resulting quickness chart, has very good potential as a tool for handling qualities estimation by revealing the extra pilot workload required to fly an inferior helicopter through the same manoeuvre. However, the results are only valid if the calculations have been made over a single pilot input or pulse which is devoid of sophisticated control overshoots, that is, the particular task must be performed open loop.

4.2.1 Open Loop Requirements For Valid Quickness Value Calculations

Helicopter inverse simulation is essentially a closed loop domain and can be viewed as an ideal pilot executing the perfect control displacements to constrain the vehicle to a prescribed flight path. Initially it seems that this contradicts the open loop requirements described above, but the problem is resolved when it is realised that the results from inverse simulation are equally valid for closed or open loop simulation. This is demonstrated by recalling that forward simulation using the results obtained from an inverse simulation run, reproduces the originally defined flight path, and leads to the conclusion that inverse simulation can be used for open loop quickness value calculations, provided the pilot input analysed is a simple pulse with no compensating or corrective overshoots.

4.3 Lateral Cyclic Pitch Frequency Chart

The data in Figure 11 is presented for three varying aggression side-steps for a single Lynx configuration. If Lynx-2 is simulated using the same three side-step MTEs, Table 1, and the calculated quickness values are superimposed on Figure 11, the resulting chart is not as straight-forward, and is somewhat cluttered with data points, Figure 14. In order to clarify this and perhaps present the information in a more revealing form, a frequency chart can be drawn, which illustrates the rate of occurrence of control activity close to the available limit, Figure 15. This is quite a useful measure of workload for a single helicopter, and when used as a tool for comparison, has the capacity to identify the inferior configuration. Figure 15 illustrates this by unambiguously identifying Lynx-2 as an inferior configuration as it has a higher frequency of control inputs that exceed sixty percent of the maximum control limit. Although the side-steps are classified into categories of varying aggression, they are all severe manoeuvres and even the most experienced of pilots would be working intensely to conform to the parameters imposed on the manoeuvres. It is therefore not unsurprising that Lynx-1 also has a quite a high frequency of relatively large control inputs.

5. The Lateral Cyclic Stick Displacement Quickness Parameter ($Q_{\eta 1c}$)

Pilot workload and hence handling qualities can be monitored by a second quickness parameter known as the stick displacement quickness parameter ($Q_{\eta 1c}$). Helinv is capable of generating the pilot stick displacement time-histories which can be integrated, and the quickness parameters obtained simply using the following equation:

$$\text{Lateral Cyclic Stick Displacement Quickness } (Q_{\eta 1c}) = \frac{\eta_{1cpk}}{\Delta I \eta_{1c}} \qquad (4)$$

where η_{1cpk} is the peak stick displacement. The denominator of the equation, is analogous to the lateral cyclic pitch quickness parameter as it employs the integral of stick displacement, which was found to be more appropriate when plotting the quickness charts.

5.1 Comparison of Lateral Cyclic Stick Displacement Quickness for Varying Aggression Rapid Side-step MTEs

It is typical that the results from the lateral stick displacement studies should confirm those in the lateral cyclic pitch simulations, and identify the manoeuvre that is most difficult to fly from a pilot point of view. Side-step three is again seen as the manoeuvre that produces the greatest lateral cyclic stick displacements, Figure 16c, and this is confirmed on the quickness chart, Figure 17, as it produces the highest quickness values. This chart follows the general hyperbolic trend, that is, as the severity of the manoeuvre is increased the quickness values move upward and to-the-left, with gentle manoeuvres producing a downward and to-the-right inclination. Contour lines corresponding to 50% and 100% of the maximum lateral stick limit are also annotated on the diagram to give a clear indication of the severity of the manoeuvres.

5.2 Comparison of Lateral Cyclic Stick Displacement Quickness For Two Lynx Configurations

Further substantiation of degraded handling qualities in the second Lynx configuration is evident time-histories presented in Figures 18a and b, and in the stick displacement quickness chart, Figure 19. The points on the quickness chart appear in pairs, with the highest quickness values for each helicopter configuration associated with the second and third control inputs respectively. This leads to the conclusion, (which is more difficult to deduce from the lateral cyclic pitch quickness chart), that the control input from trim to initiate the manoeuvre, and the final input to terminate the side-step are not as severe as the stick displacements which occur in between. Once more, it is Lynx-2 that is clearly identified as the inferior configuration as it produces quickness values that approach the lateral cyclic limits, while Lynx-1 still has a higher percentage of control available, hence reducing the workload on the pilot leaving more time to perform other non-piloting tasks.

In keeping with the previous study performed on the lateral cyclic pitch, the side-step lateral cyclic stick quickness values for both Lynx configurations and all three side-steps were plotted on the same chart, Figure 20. It is still possible to identify the hyperbolic trend, but it is not a straightforward matter to establish which of the two vehicles demands a higher workload from the pilot. The bar chart shown in Figure 21 shows the frequency of lateral cyclic stick displacement as a percentage from of the total stick displacement available. It is possible to say that Lynx-2 demands a higher workload, and presents itself as being greatly inferior to Lynx-1. It has been illustrated that the lateral cyclic stick displacement quickness parameter is another useful method of identifying manoeuvres of high workload, and distinguishing between helicopters of dissimilar configuration pinpointing the inferior aircraft.

6. Preliminary Study On Control System Interference

The primary control exercised in the rapid side-step MTE is lateral cyclic, in other words the control which permits the pilot to generate rolling moments about the aircraft's centre of gravity. For this reason it has been the lateral cyclic pitch and lateral cyclic stick displacement which has been analysed in this report, and a more comprehensive treatment of the lateral cyclic channel is given in Appendix A. Since the inverse simulation package at Glasgow incorporates the ability to engage a Stability and Control Augmentation System (SCAS) while simulating manoeuvres, it was decided to conduct an initial study into how the SCAS effects pilot workload. Complimentary to this, the effects of altering the value of the lateral cyclic actuator constant, τ_{c2} (see Appendix A), were also investigated, the results of which are presented below.

6.1 Effect of Using Stability and Control Augmentation System During Rapid Side-step MTE

It is highly desirable to optimise manoeuvrability and reduce pilot workload, especially if the helicopter is designed to operate in a potentially hazardous battlefield environment. One method of doing so is the application of an Automatic Flight Control System, which is composed of a Stability and Control Augmentation System (SCAS) and an autopilot. Since all of the work presented so far in this report was obtained from simulations with the SCAS switched off, it was a logical decision to investigate the effects of switching it on during execution of the rapid side-step MTE. Figures 22a and b illustrate the lateral cyclic stick displacement time-histories with the SCAS activated, and it can be seen that it has reasonable effect on the stick movement during the manoeuvre, when compared with the normal Lynx-1 stick activity shown in Figure 22a. This is confirmed on observing the quickness chart in Figure 23, where the side-step with the SCAS on yields the lowest values of quickness, suggesting less workload.

6.2 Effect of Setting Lateral Cyclic Actuator Time Constant to Zero (τ_{c2}= 0.0)

The lateral cyclic actuator time constant, (τ_{c2}) is a pure time delay between the time taken for a lateral cyclic stick input from the pilot, and the resulting change in the blade pitch angle taking place. The value of the lateral cyclic time constant in the Westland Lynx helicopter is typically around 0.125 seconds, and setting this value to zero in the first instance, essentially means that when the stick is displaced by the pilot the blade pitch will instantaneously alter according to the amount of stick input. Correspondingly this reduces the effective stick displacement required to perform a specific manoeuvre, and this can be seen in Figure 24b. The quickness values plotted on the chart, Figure 25 show this configuration to be quite effective in decreasing the pilot workload, and are similar to those results obtained with the SCAS activated.

6.3 Effect of Doubling the Lateral Cyclic Actuator Time Constant (τ_{c2}= 0.25)

It was expected that increasing the lateral cyclic actuator time constant would have the opposite effect from the previous study. The bottom diagram in Figure 24c illustrates the fact that using a lateral cyclic actuator time constant of 0.25 produces the largest stick displacements and subsequently the highest quickness values suggesting higher workloads, Figure 25. The lateral cyclic limits of the helicopter are also approached more closely, implying that this vehicle configuration would be less capable of flying similar aggressive manoeuvres than those described above.

7. Conclusions

The primary conclusions of the work presented in this paper are largely based on the objective assessment of helicopter pilot workload using the lateral cyclic pitch and lateral cyclic stick quickness parameters in conjunction with the helicopter inverse simulation package, Helinv. The work was centred on the Rapid Side-step Mission Task Element (MTE) and it was shown how this manoeuvre effectively differs from the previous side-step definition incorporated in Helinv.

The rapid side-step MTE mathematical model used to drive Helinv was successful in encompassing all of the features described by ADS-33C, and presented the user with the ability to alter various flight definition parameters that could either increase or decrease the severity of the manoeuvre. Studies were conducted firstly on three rapid side-steps of increasing aggression, and secondly on the comparison of handling qualities of two dissimilar Westland Lynx type helicopters. It was shown that the lateral cyclic pitch quickness parameter could be used to identify the manoeuvres with highest workload or the least desirable helicopter configuration, with the studies presented in this report being in accordance with those carried out previously.

The lateral cyclic stick quickness parameter was introduced and it was illustrated how this also could be used to analyse the pilot inputs and hence probable workload during the manoeuvre. The stick quickness parameter is conceivably more useful for handling qualities estimation as it reveals exactly what is happening from a pilot point of view, and can be easier to visualise, especially on the resulting cyclic stick time-histories. It is also extremely useful for identifying aggressive manoeuvres that require extensive amounts of 'overshoot', which would have the corresponding effect of increasing pilot workload. It is possible that this may present itself as another area of investigation, which can be analysed using the quickness parameters described above.

The latter minor study in the report was successful in showing the effects of introducing a Stability and Control Augmentation System, (SCAS) and on altering the time constants on the lateral cyclic actuators. The effectiveness of the SCAS was illustrated on the lateral cyclic stick quickness chart by demonstrating that when activated, the workload was reduced considerably.

Reducing the actuator time constant to zero presented a similar situation to the activation of the SCAS and indeed yielded values close to those obtained with the SCAS engaged. The resulting quickness chart confirmed the lateral cyclic stick time-history results obtained, as the normal Lynx configuration had values that separated the actuator time constant being set to zero and to double its' usual value. Simulating the manoeuvre with the increased actuator time had the effect of increasing workload, which was represented by the quickness values moving towards the cyclic stick limit on the chart.

Therefore it does appear from this work that using the lateral cyclic quickness parameters can be a successful method of executing an initial handling qualities estimation exercise, provided of course that the helicopter mathematical model is of suitable fidelity and the MTE is capable of representing the actual manoeuvre.

References

1. Cooper, G. E., Harper, Jr., R. P. "The Use of Pilot Rating in the Evaluation of Aircraft Handling Qualities." NASA TN D-5153.

2. Anon., "Aeronautical Design Standard, Handling Qualities Requirements for Military Rotorcraft." ADS-33C, August 1989.

3. Thomson, D. G., Bradley, R., "Development and Verification of an Algorithm for Helicopter Inverse Simulation." Vertica, Vol. 14, No. 2, May 1990.

4. Thomson, D. G., Bradley, R., "Mathematical Definition of Helicopter Manoeuvres." Department of Aerospace Engineering, University of Glasgow, Internal Report No. 9225, June 1992.

5. Thomson, D. G., Bradley, R., "Validation of Helicopter Mathematical Models by Comparison of Data from Nap-of-the-Earth Flight Tests and Inverse Simulations." Paper No. 78, Proceedings of the 14th European Rotorcraft Forum, Milan, Italy, September 1988.

6. Thomson, D. G., Bradley, R., "The Contribution of Inverse Simulation to the Assessment of Helicopter Handling Qualities." Paper 7.3.2, Proceedings of the 19th ICAS Conference, Anaheim USA, September 1994.

Appendix A

The Lateral Cyclic Channel

The most common method of applying cyclic pitch is through the swashplate, which is basically a method of transferring a pilot input into a movement at the rotor hub consequently directing the rotor thrust vector and moving the aircraft. Lateral cyclic is one of four possible controls that the pilot utilises in order to manoeuvre the helicopter in the required manner, and is explained in a mathematical format below.

The relationship between lateral cyclic pitch, i.e. at the swashplate and the lateral cyclic stick input from the pilot is given by:

$$\theta_{1cp}^{*} = g_{1c0} + g_{1c1}\,\eta_{1c}$$

where,

θ_{1c}^{*} is the cyclic pitch before mixing,

g_{1c0} and g_{1c1} are cyclic stick gearing constants and

η_{1c} is the lateral cyclic stick displacement ($0 \leq \eta_{1c} \leq 1$)

The SCAS contribution to the lateral cyclic channel is obtained via feedback from the roll-rate, p and roll attitude, ϕ of the helicopter. An additional feed-forward term based on the position of the cyclic stick is also included to permit enhanced vehicle response to a given lateral cyclic stick input.

Therefore the lateral cyclic contribution from the SCAS, θ_{1ca}^{*} is obtained from:

$$\theta_{1ca}^{*} = k_{\phi}\,\phi + k_{p}\,p + k_{1c}\,(\eta_{1c} - \eta_{1c0})$$

where,

k_{ϕ} is a proportional feedback gain,

k_{p} is a derivative action feedback gain,

k_{1c} is the feed-forward gain and

η_{1c0} is the reference pilot stick position, $(0 \leq \eta_{1c0} \leq 1)$

The transfer function of the combined pilot and SCAS is given by:

$$\frac{\theta_{1c}^{*}}{\theta_{1cp}^{*} + \theta_{1ca}^{*}} = \frac{1}{1 + \tau_{c2}\,s}$$

where τ_{c2} is the lateral cyclic actuator time constant

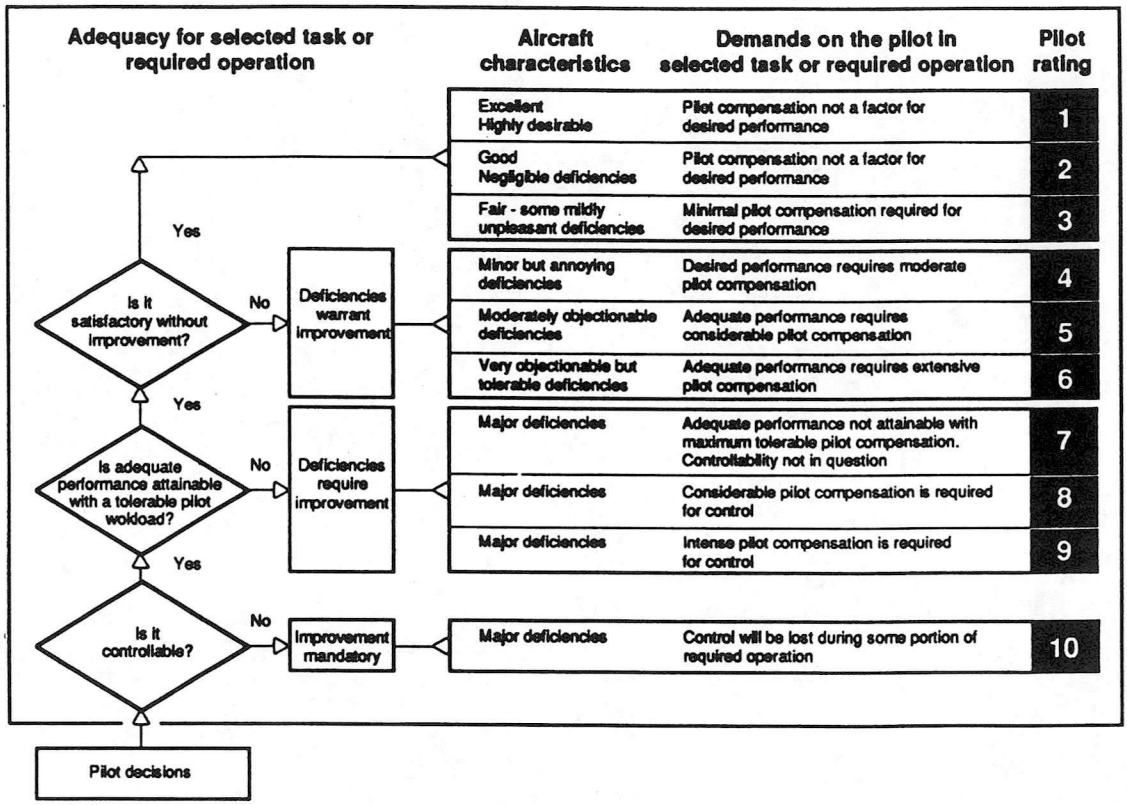

Figure 1 The Cooper-Harper Handling Qualities Rating Scale, [1]

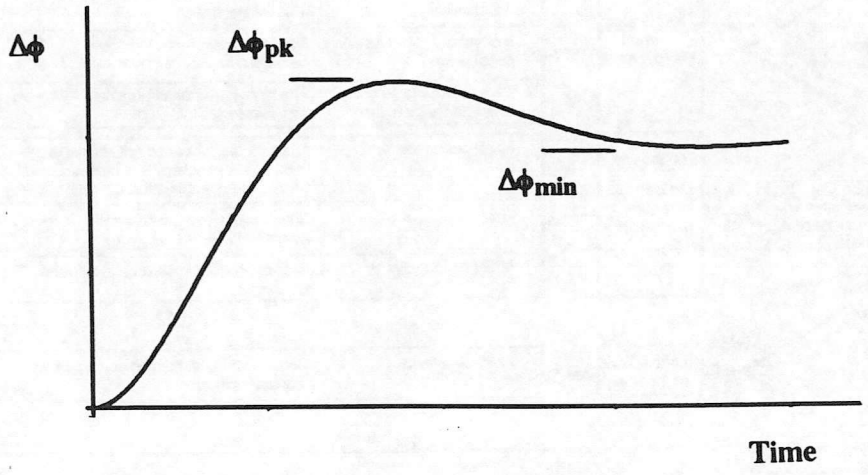

Figure 2 Illustration of $\Delta\phi_{pk}$ and $\Delta\phi_{min}$, [7]

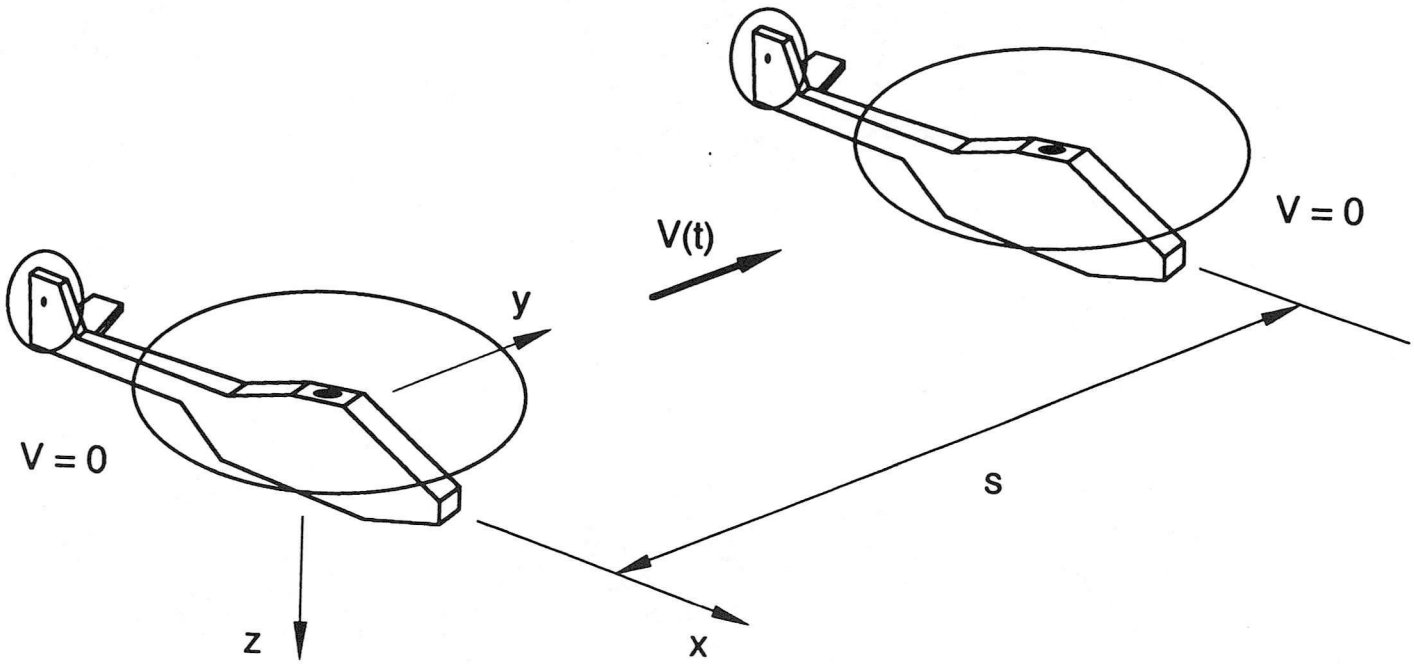

Figure 3 **Illustration of Rapid Side-step Mission Task Element (MTE), [7]**

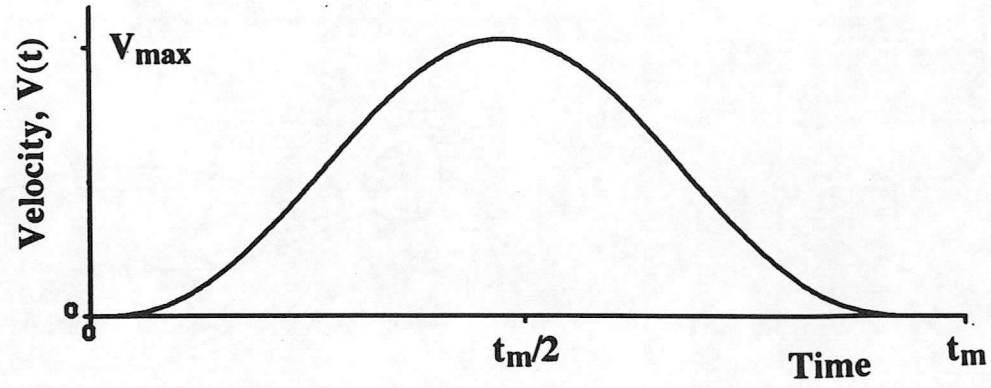

Figure 4a Global polynomial velocity profile, [7]

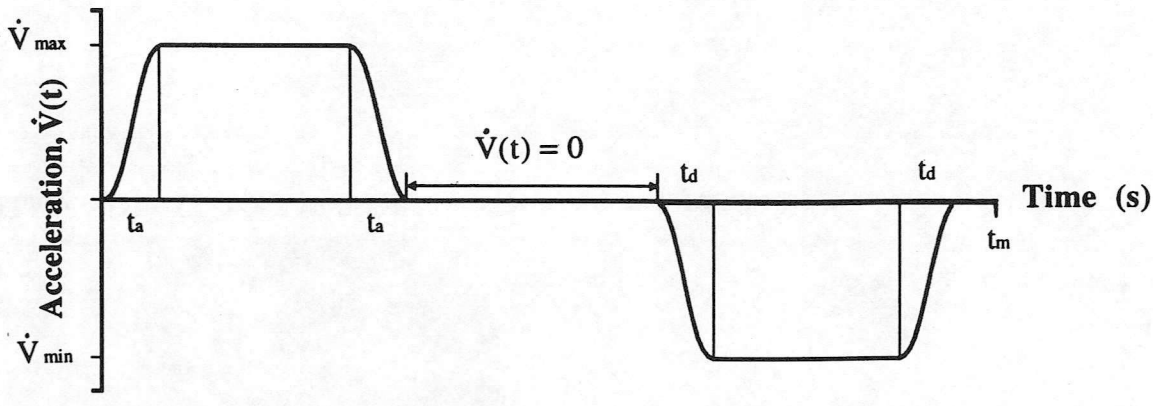

Figure 4b Acceleration profile of piecewise polynomial

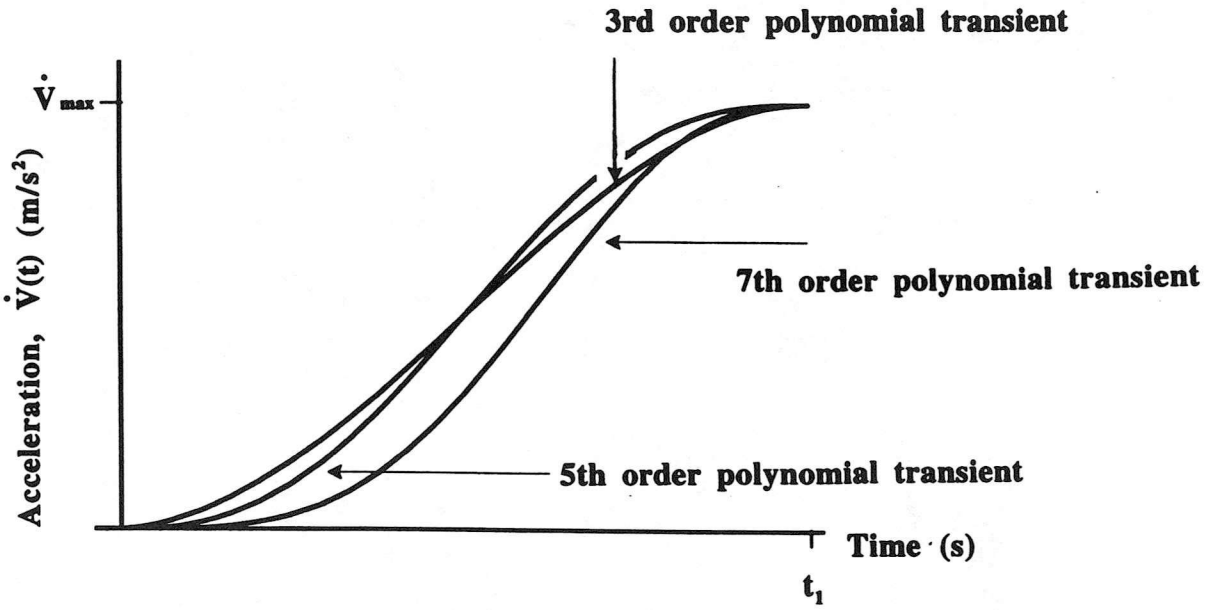

$$\dot{V}(t) = \left[-2\left(\frac{t}{t_1}\right)^3 + 3\left(\frac{t}{t_1}\right)^2\right]\dot{V}_{max} \qquad \text{3rd order polynomial transient}$$

$$\dot{V}(t) = \left[6\left(\frac{t}{t_1}\right)^5 - 15\left(\frac{t}{t_1}\right)^4 + 10\left(\frac{t}{t_1}\right)^3\right]\dot{V}_{max} \qquad \text{5th order polynomial transient}$$

$$\dot{V}(t) = \left[\frac{10}{3}\left(\frac{t}{t_1}\right)^7 - 14\left(\frac{t}{t_1}\right)^5 + \frac{35}{3}\left(\frac{t}{t_1}\right)^4\right]\dot{V}_{max} \qquad \text{7th order polynomial transient}$$

Figure 5 3rd, 5th and 7th order transient functions for piecewise polynomial

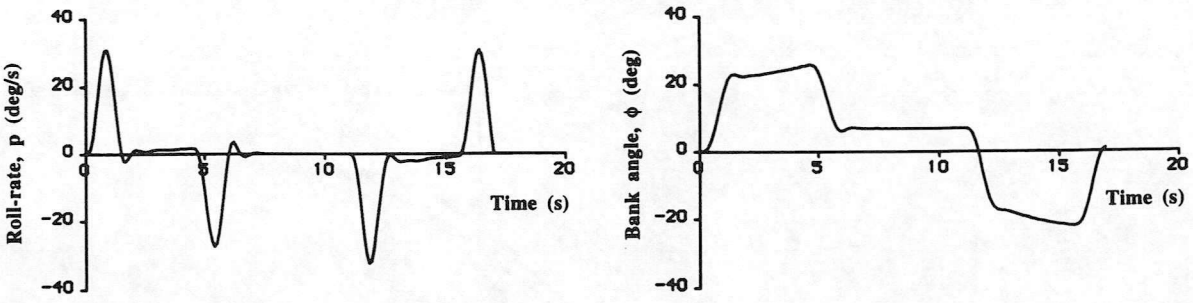

(a) Side-step 1

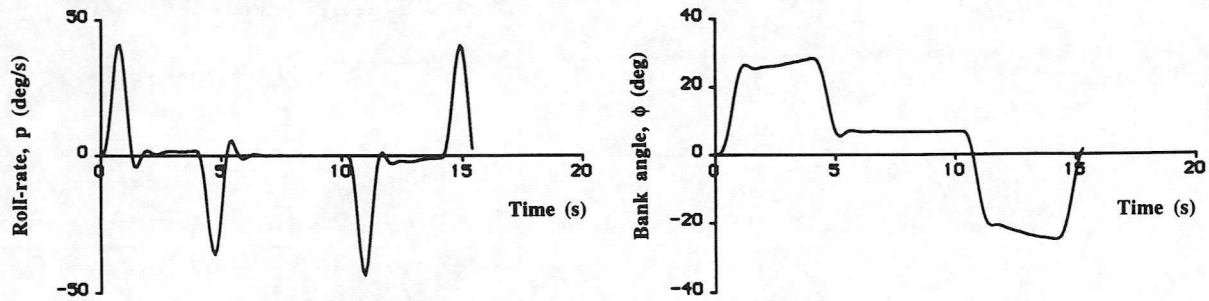

(b) Side-step 2

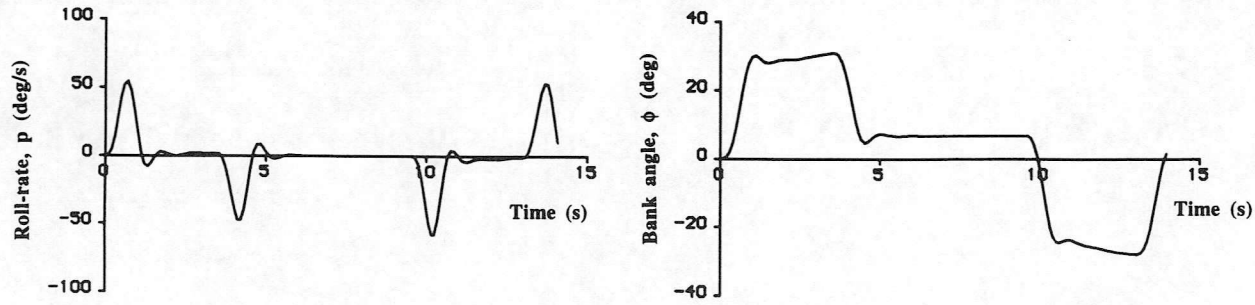

(c) Side-step 3

Figure 6 **Roll-rate, p and roll angle, ϕ time-histories for three rapid side-step MTEs**

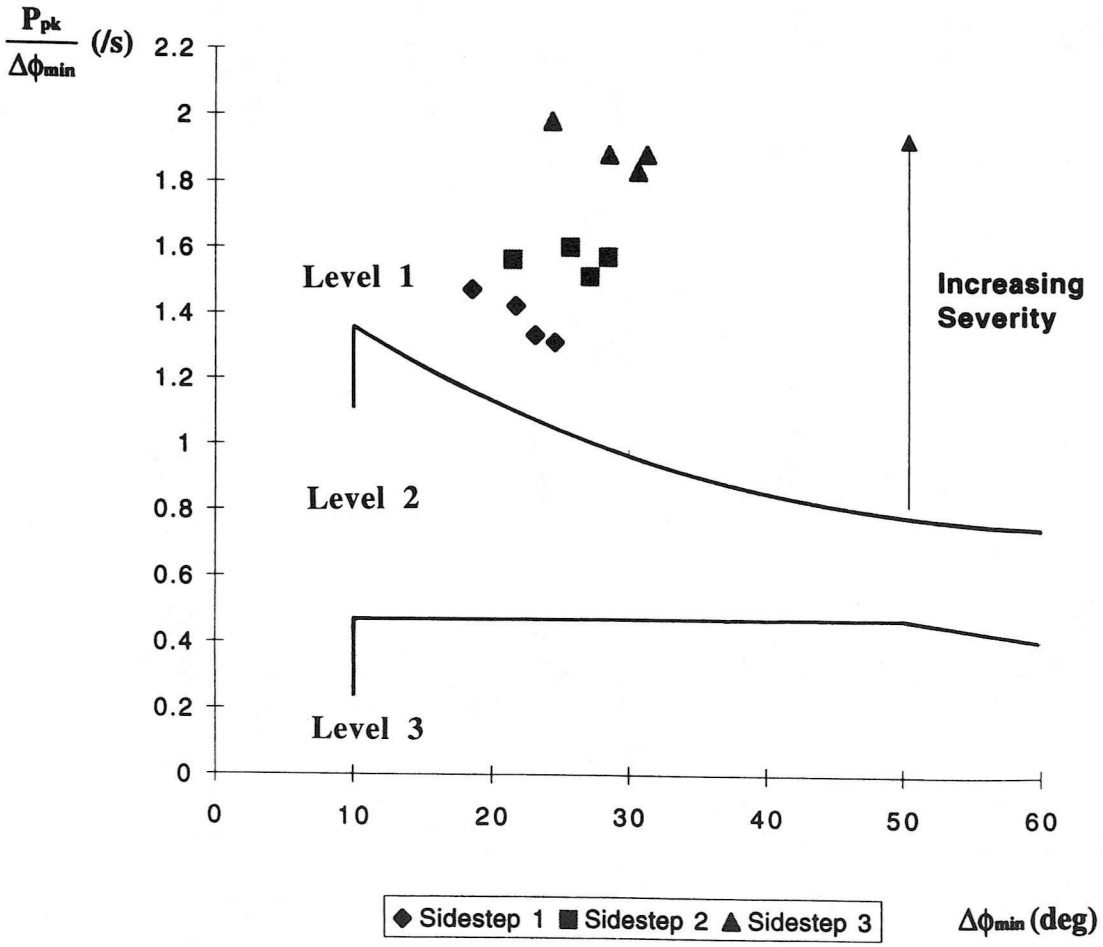

Figure 7 Roll quickness chart calculated using Figure 6 time-histories

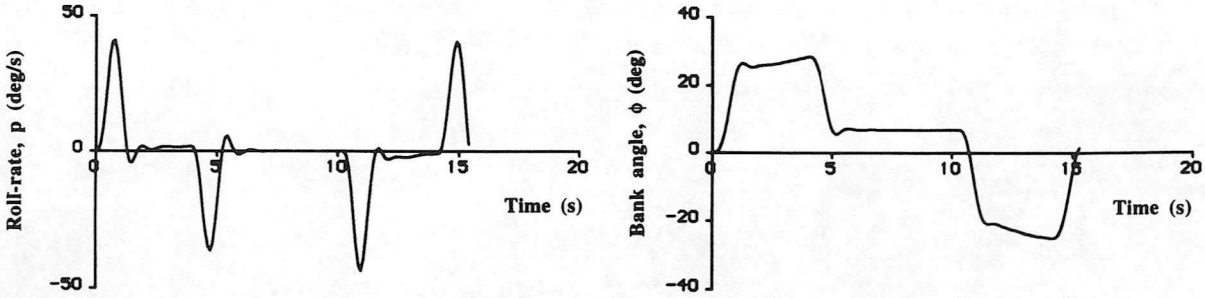

(a) Lynx-1

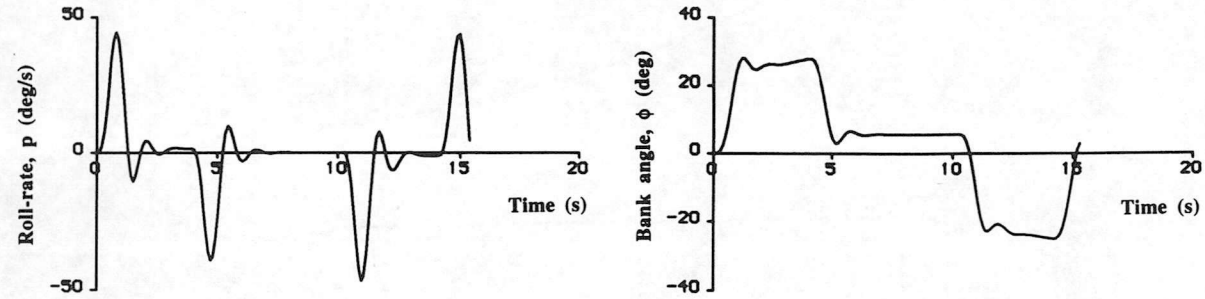

(b) Lynx-2

Figure 8 Roll-rate, p and roll angle, ϕ time-histories for the two dissimilar Lynx configurations

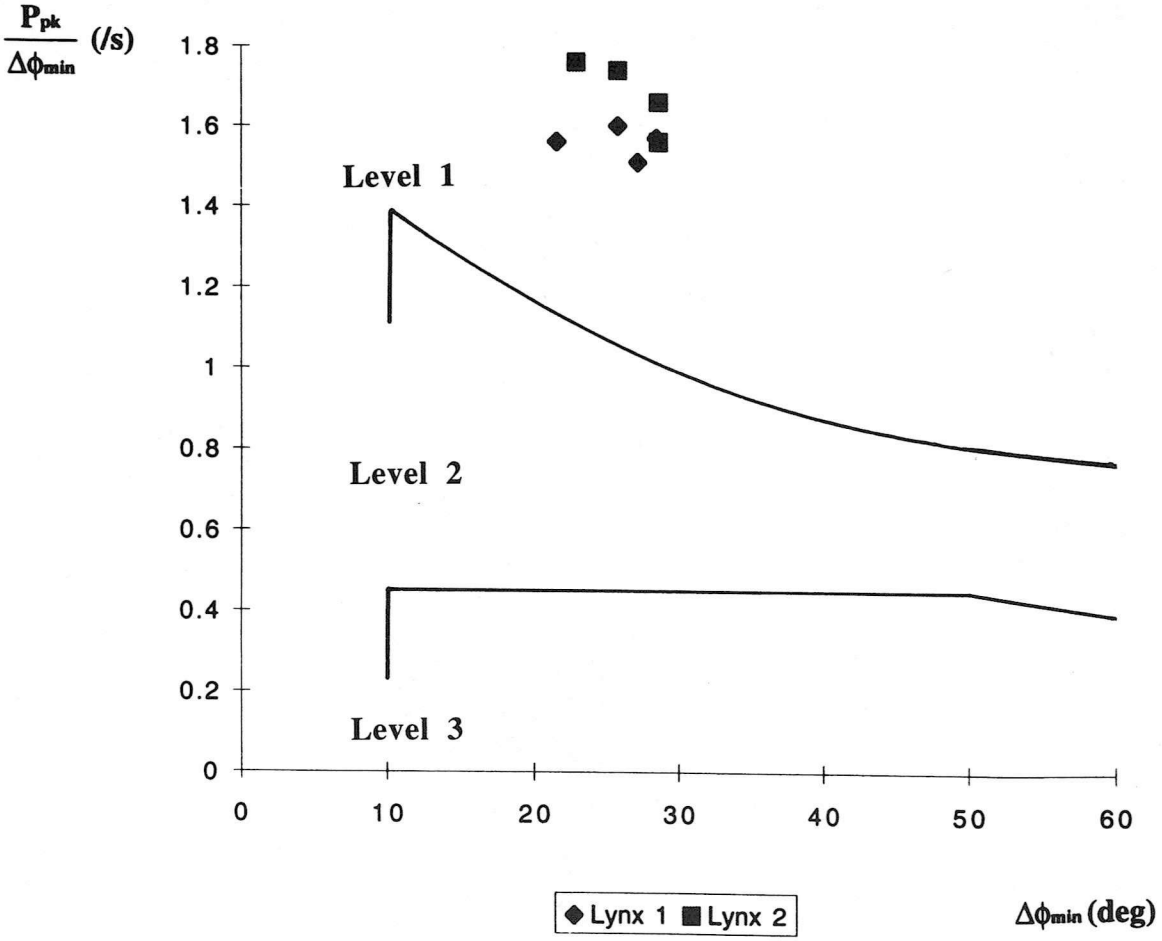

Figure 9 **Roll quickness chart calculated from Figure 8 time-histories**

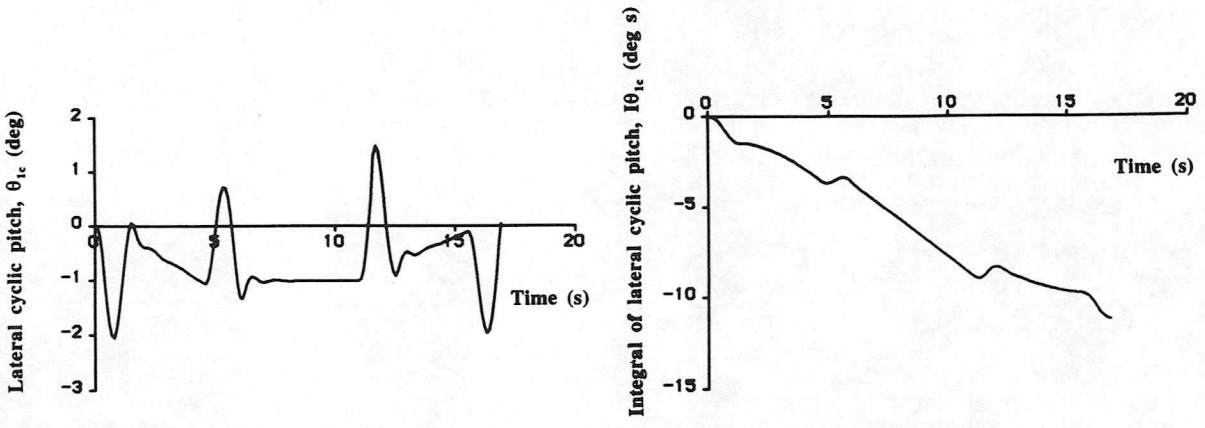

(a) Side-step 1

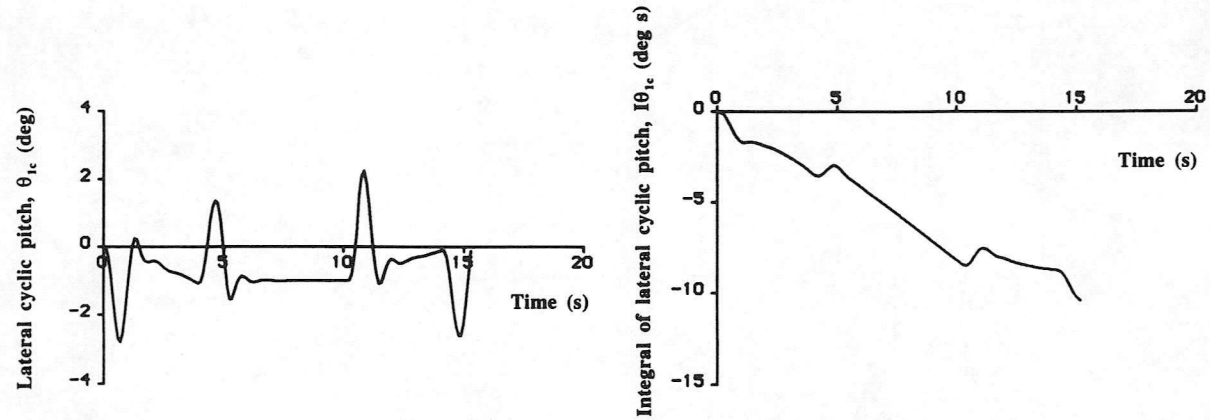

(b) Side-step 2

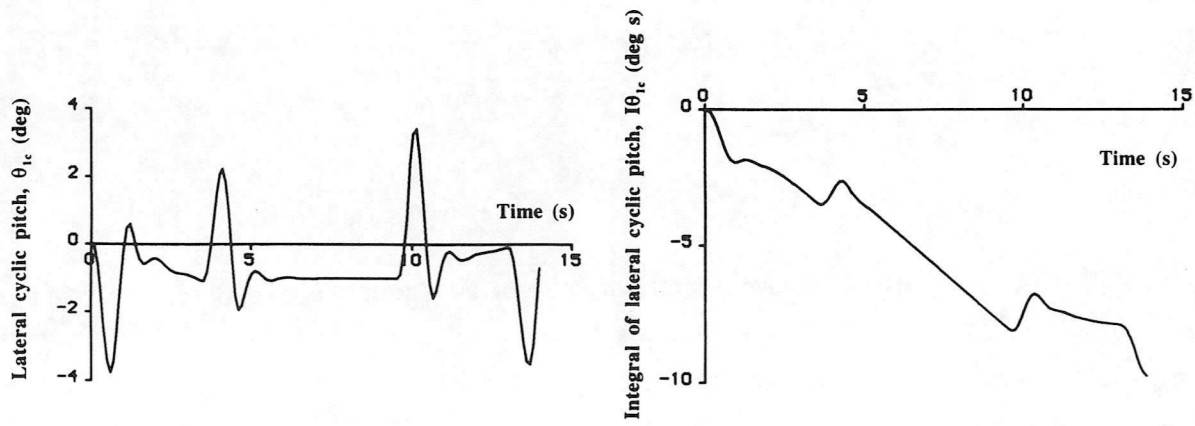

(c) Side-step 3

Figure 10 Lateral cyclic pitch, θ_{1c} and integral of lateral cyclic pitch, $I\theta_{1c}$ time-histories for the three rapid side-step MTEs

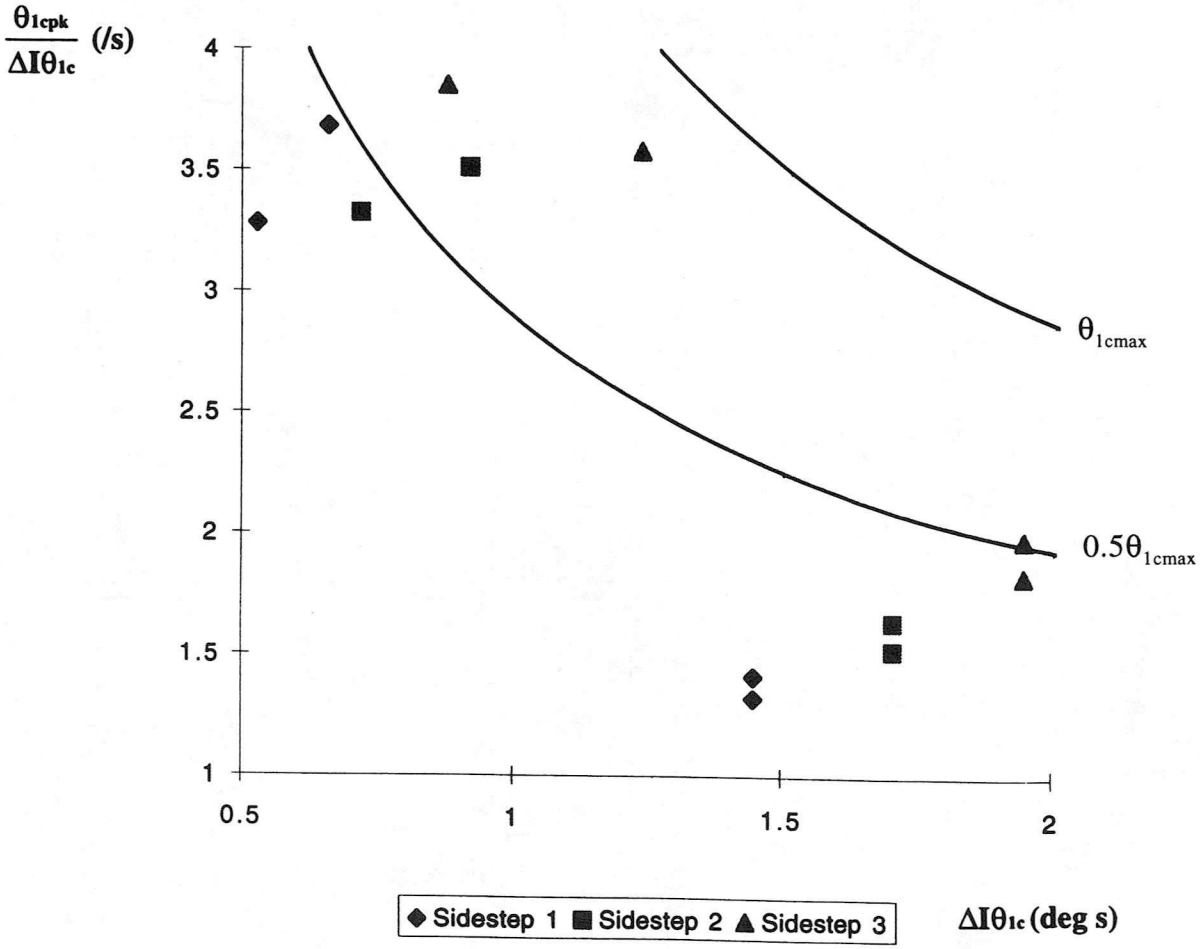

Figure 11 **Lateral cyclic pitch quickness chart calculated from Figure 10 time-histories**

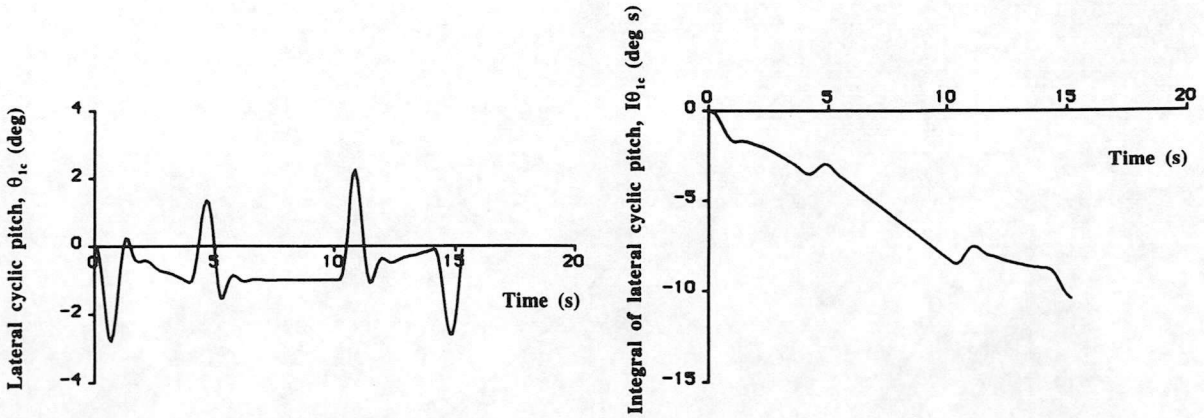

(a) Lynx-1

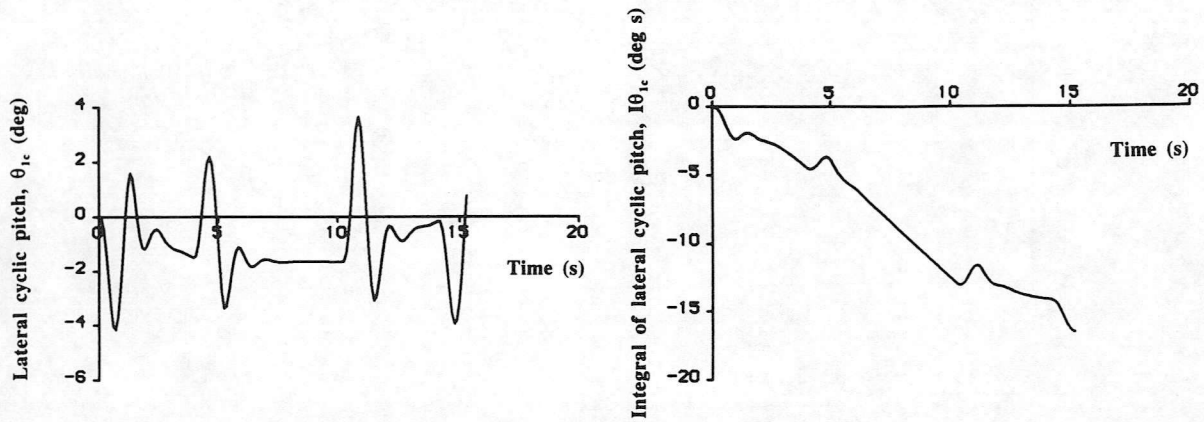

(b) Lynx-2

Figure 12 Lateral cyclic pitch, θ_{1c} and integral of lateral cyclic pitch, $I\theta_{1c}$ for the two dissimilar Lynx configurations

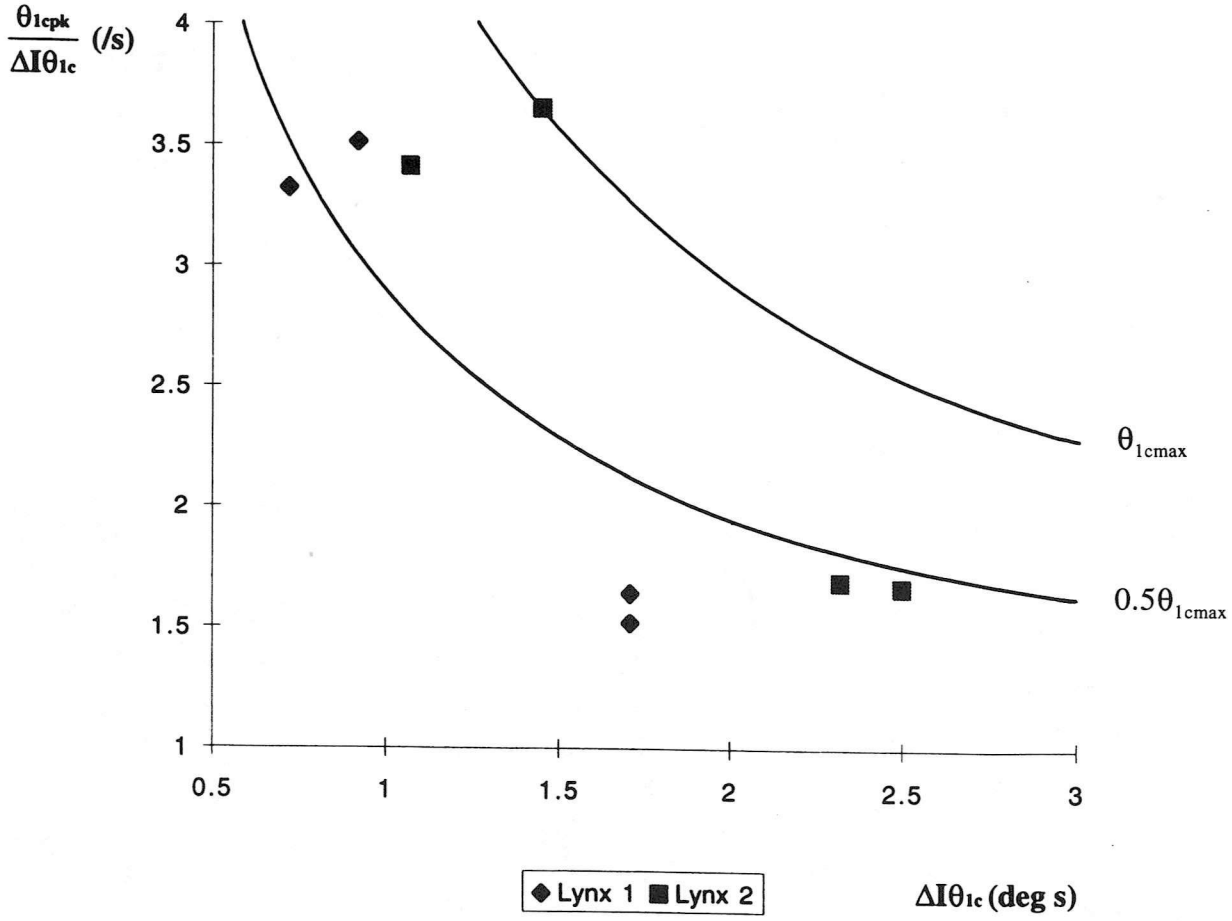

Figure 13 **Lateral cyclic pitch quickness chart calculated from Figure 12 time-histories**

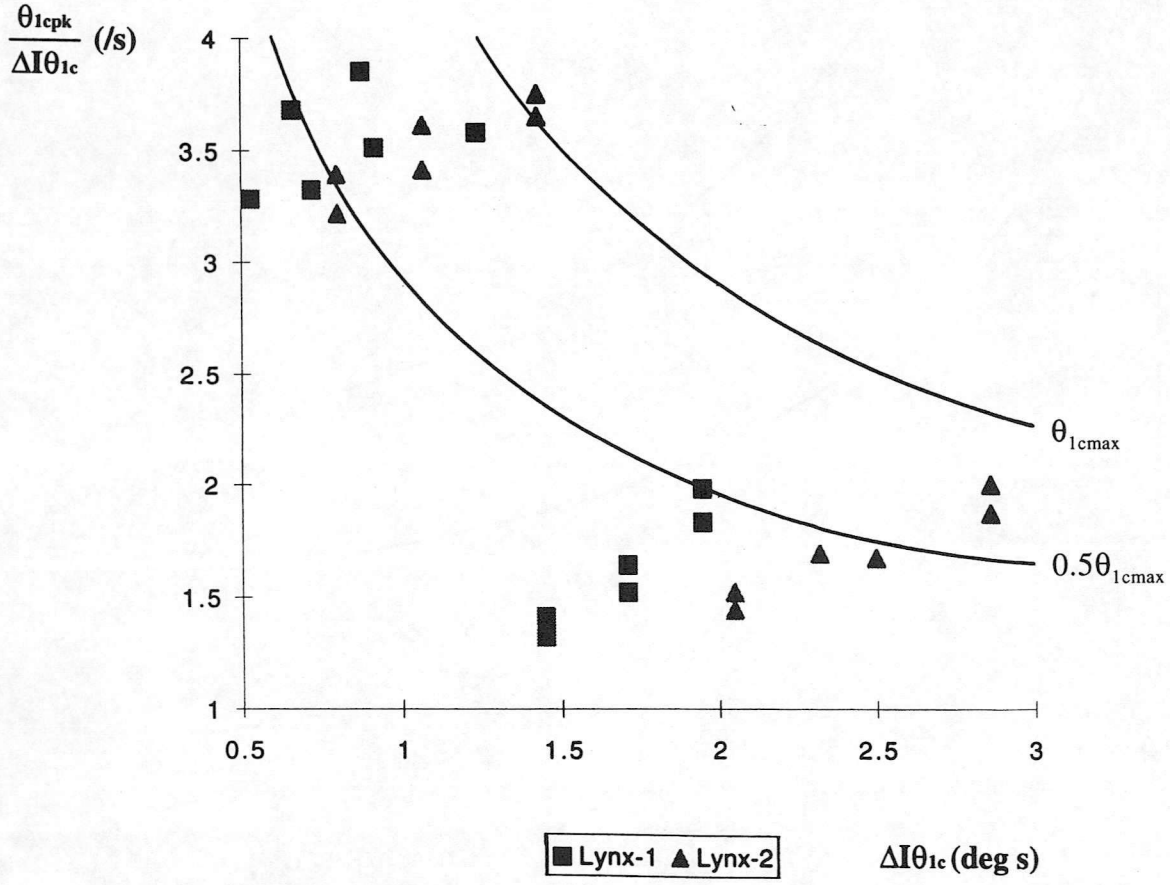

Figure 14 **Lateral cyclic pitch quickness chart for both Lynx configurations and all three rapid side-step MTEs**

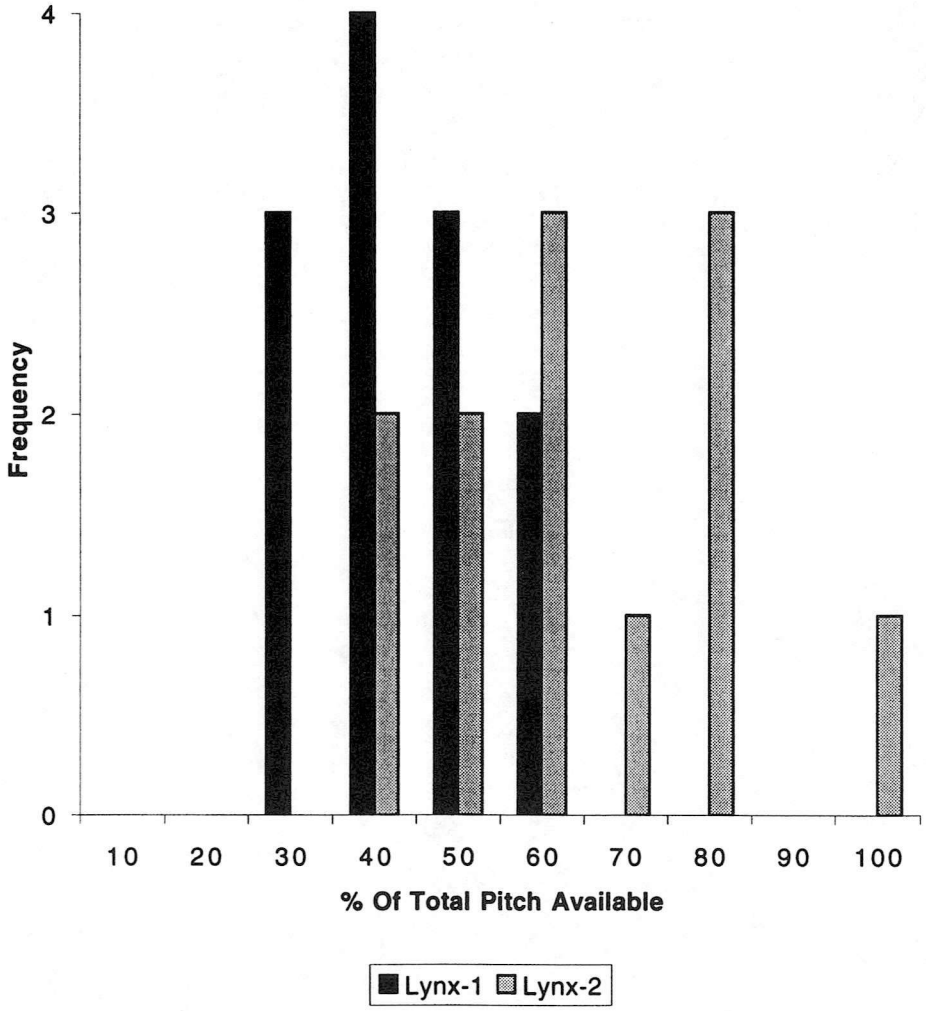

Figure 15 Lateral cyclic pitch frequency chart

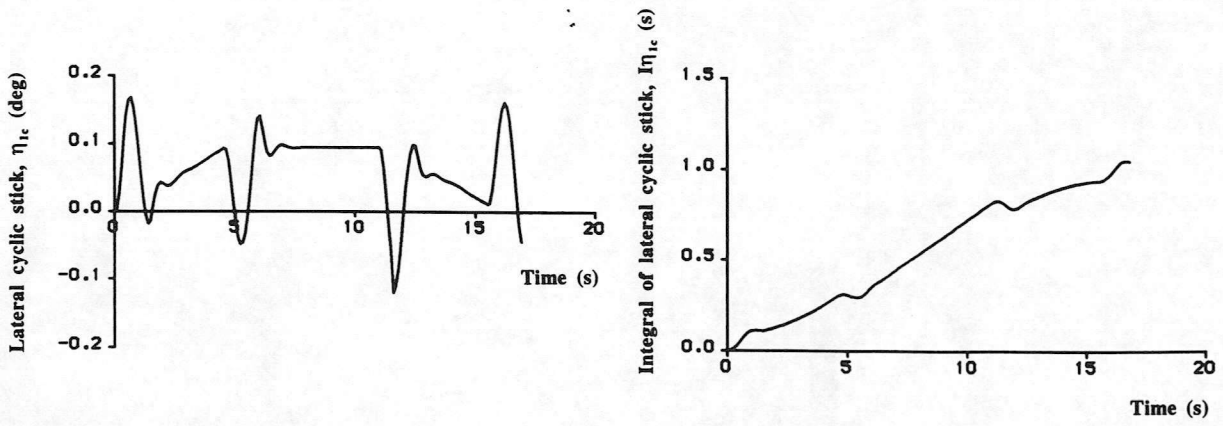

(a) Side-step 1

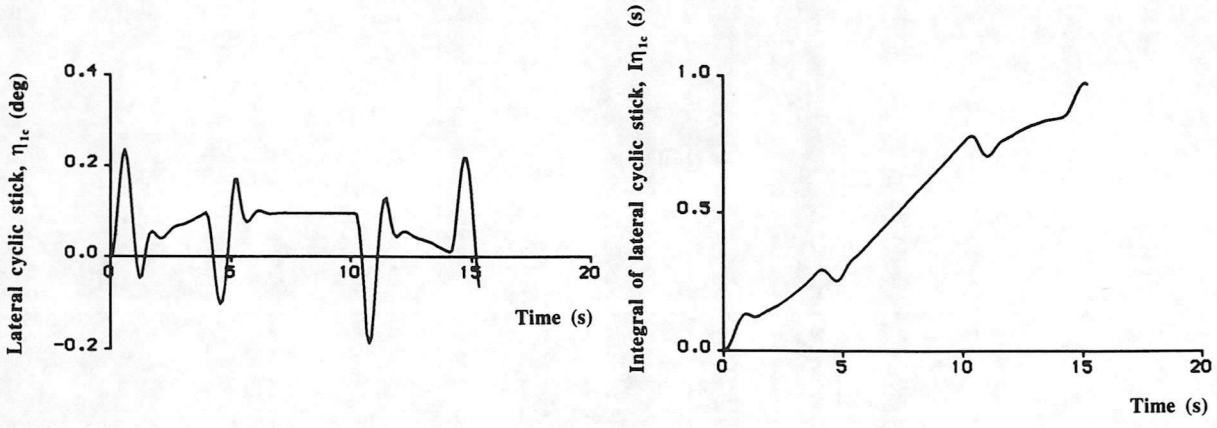

(b) Side-step 2

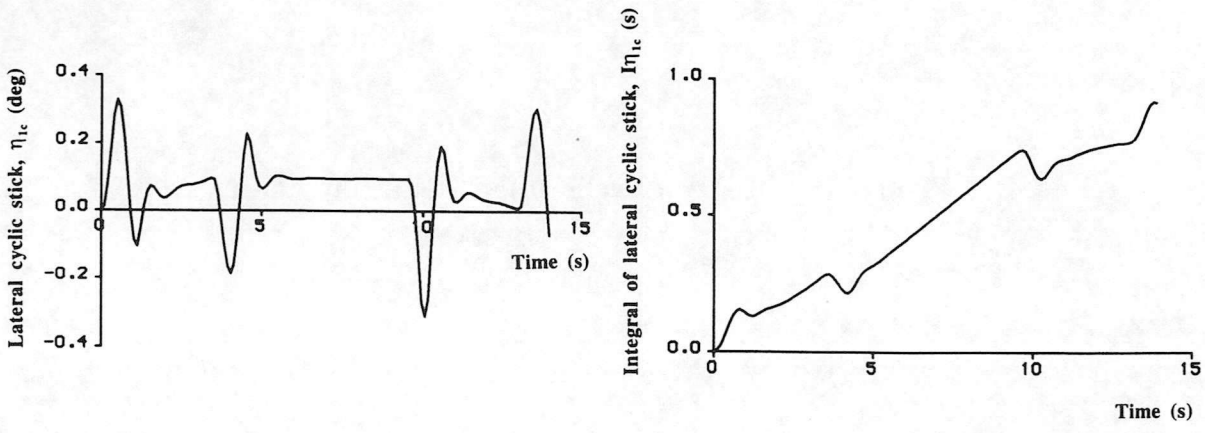

(c) Side-step 3

Figure 16 Lateral cyclic stick displacement, η_{1c} and integral of lateral cyclic stick, $I\eta_{1c}$ time-histories for the three rapid side-step MTEs

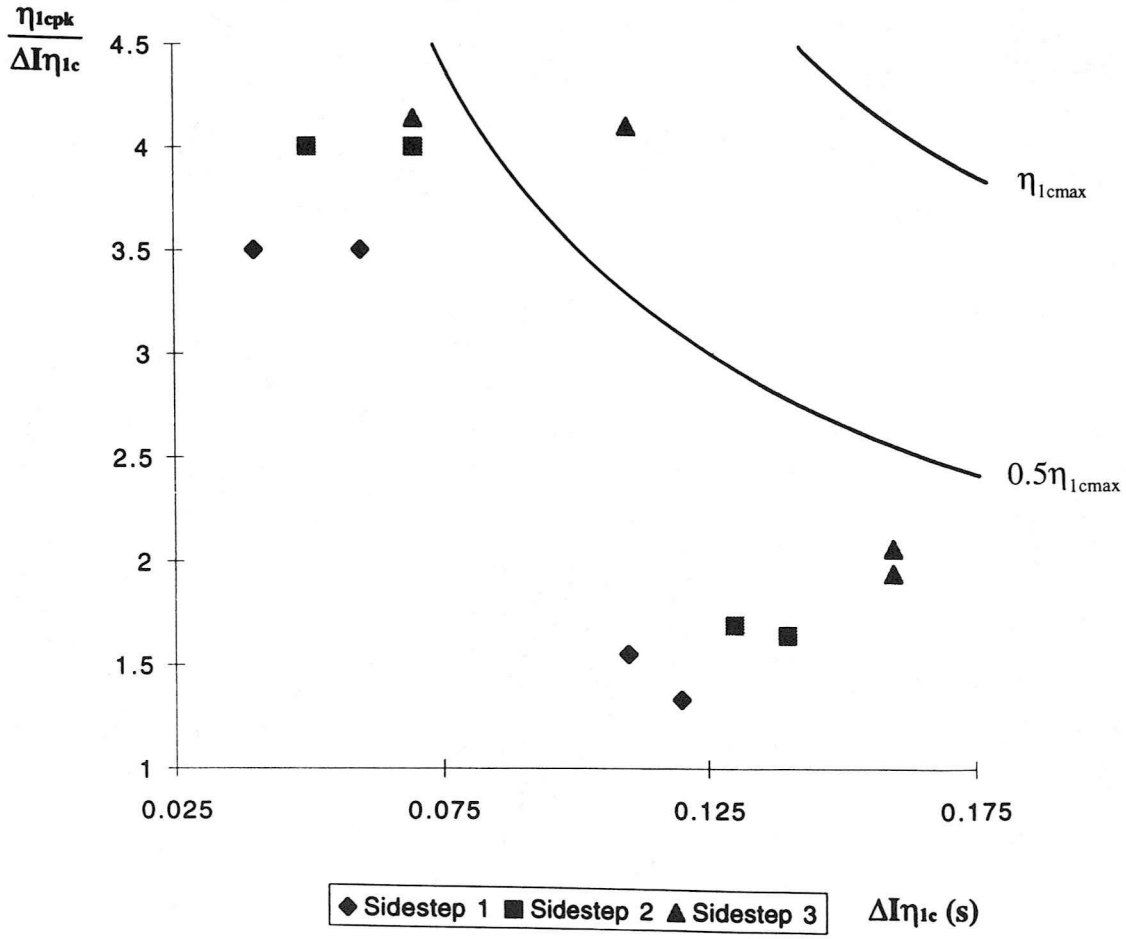

Figure 17 **Lateral cyclic stick displacement quickness chart calculated from Figure 16 time-histories**

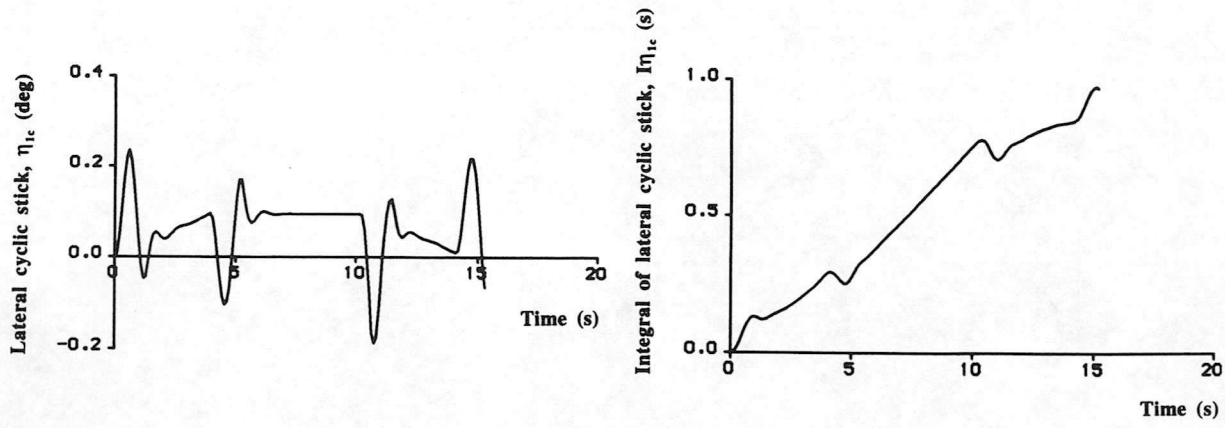

(a) Lynx-1

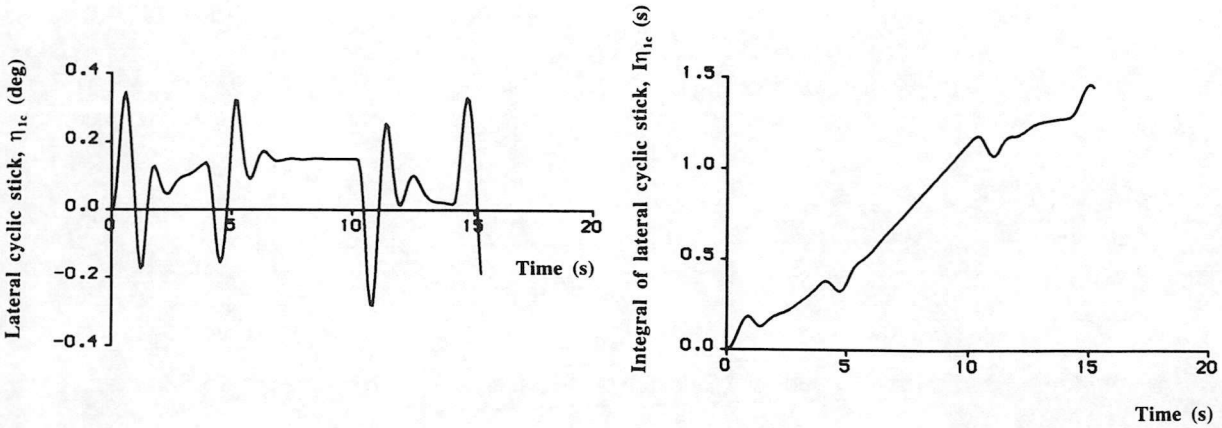

(b) Lynx-2

Figure 18 **Lateral cyclic stick displacement, η_{1c} and integral of lateral cyclic stick, $I\eta_{1c}$ time-histories for the two dissimilar Lynx configurations**

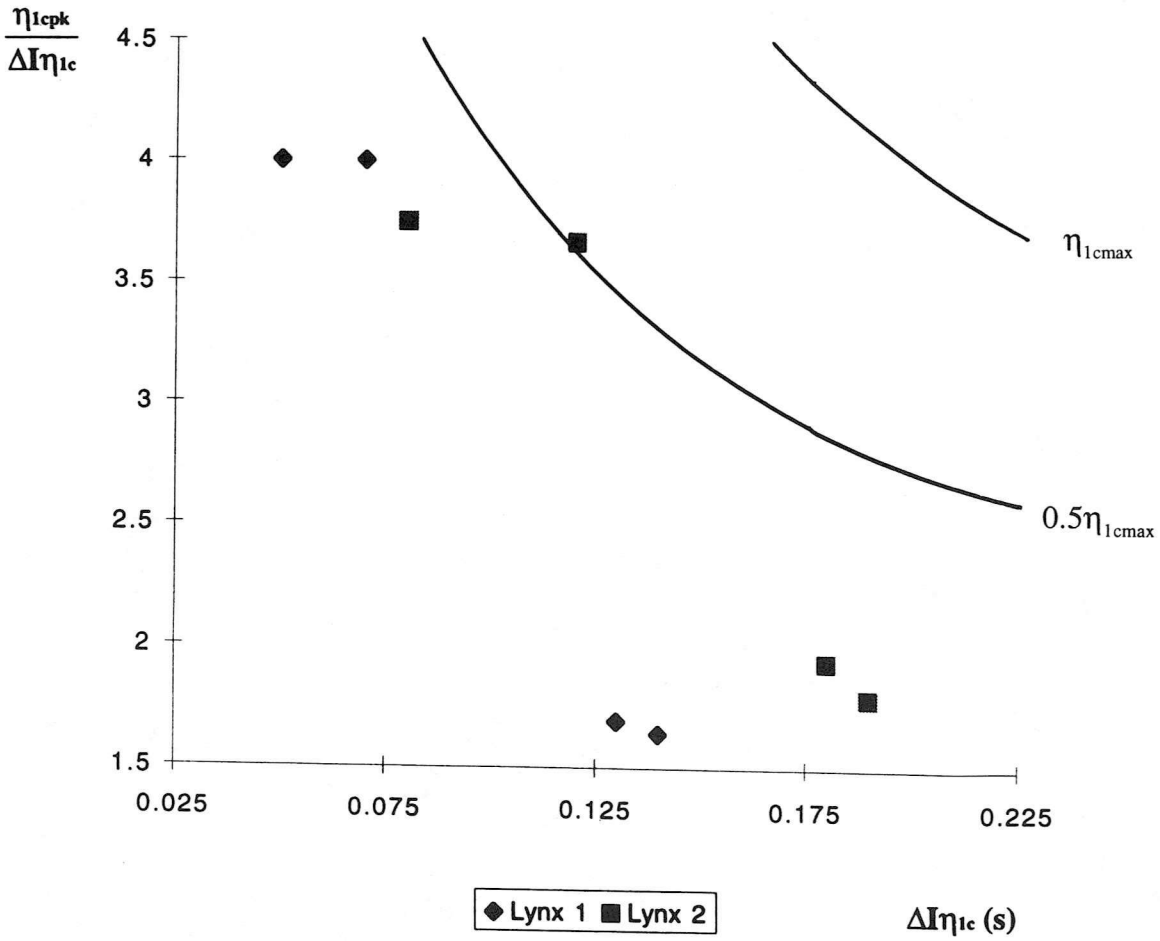

Figure 19 **Lateral cyclic stick quickness chart calculated from Figure 18 time-histories**

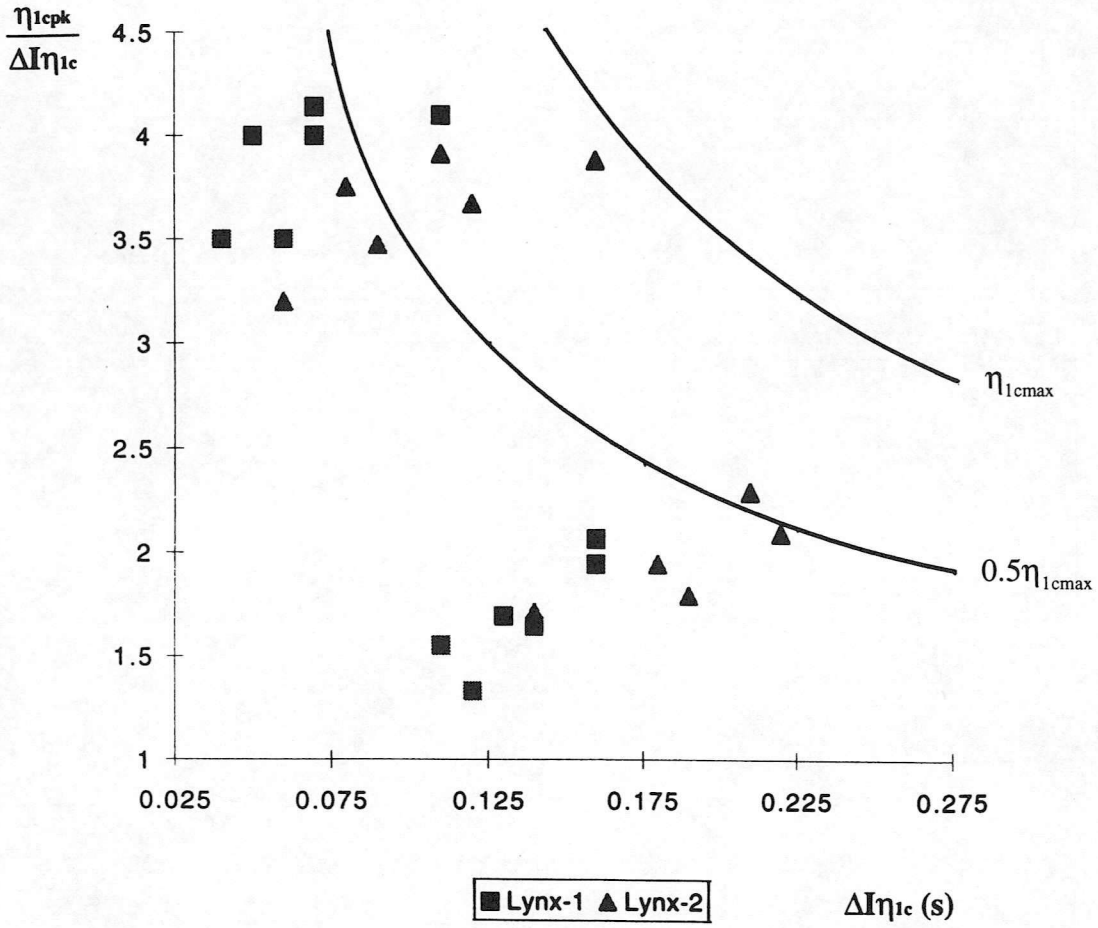

Figure 20 Lateral cyclic stick displacement quickness chart for both Lynx configurations and all three rapid side-step MTEs

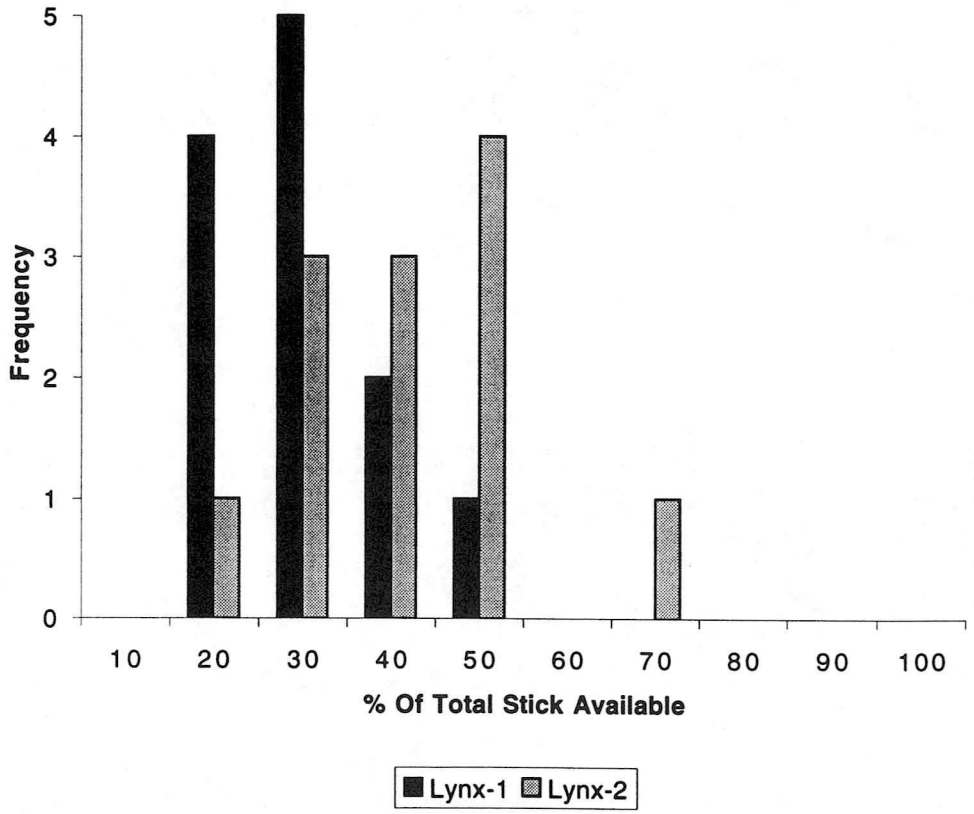

Figure 21 Lateral cyclic stick frequency chart

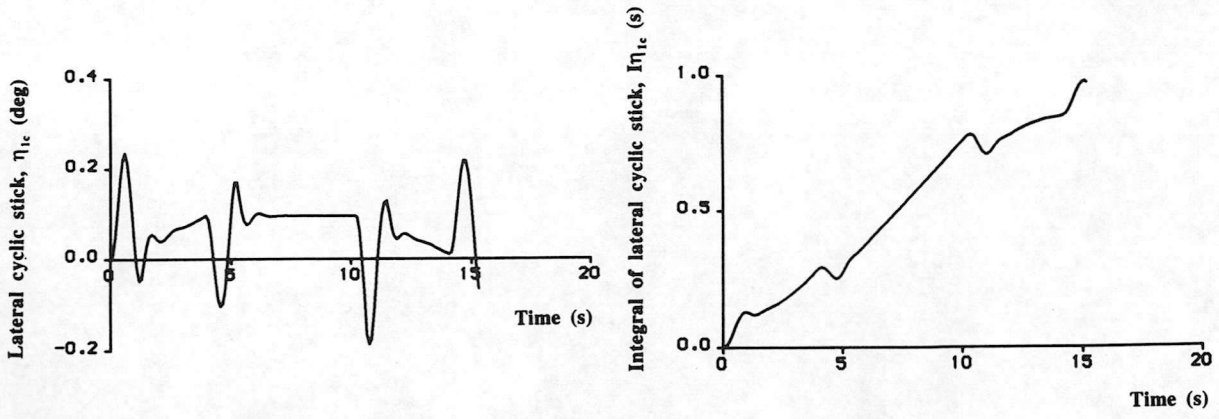

(a) Stability and Control Augmentation System (SCAS) Off

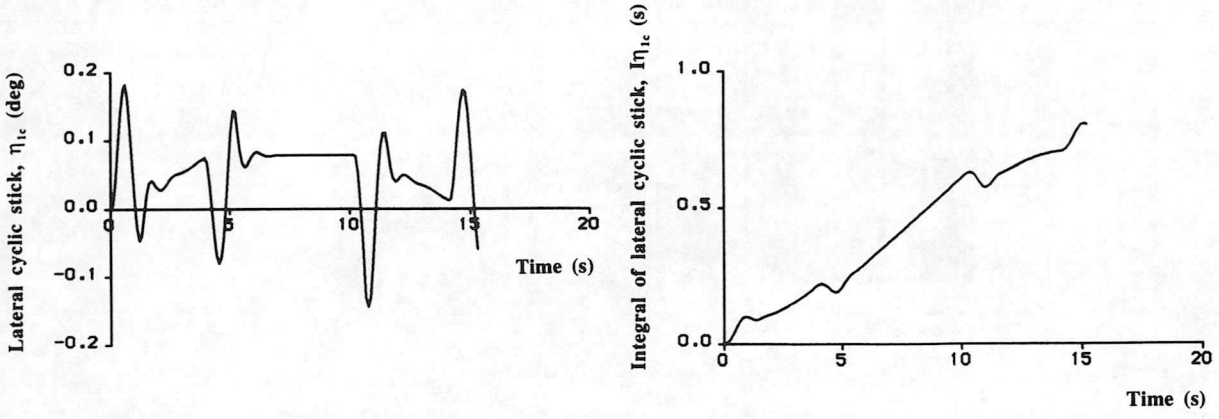

(b) Stability and Control Augmentation System (SCAS) On

Figure 22 Lateral cyclic stick displacement, η_{1c} and integral of lateral cyclic stick, $I\eta_{1c}$ time-histories for Lynx-1

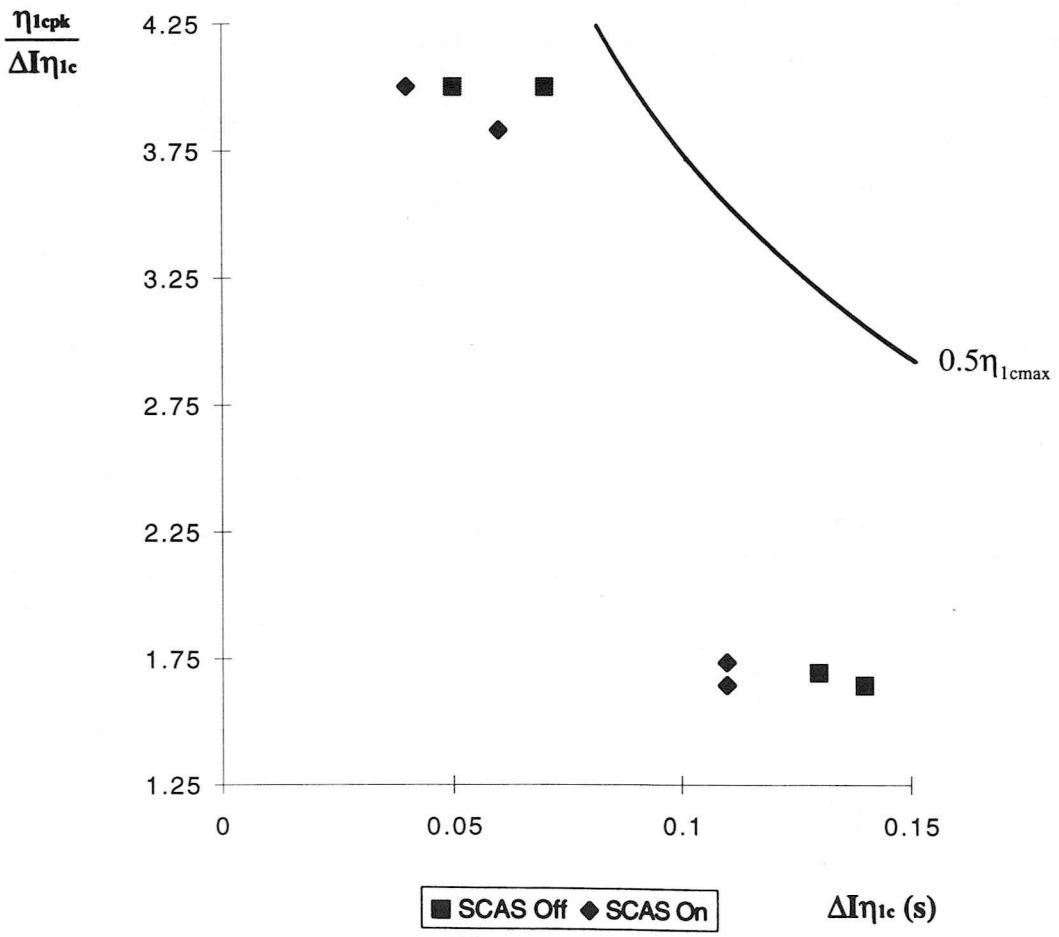

Figure 23 Lateral cyclic stick displacement quickness chart calculated from Figure 22 time-histories

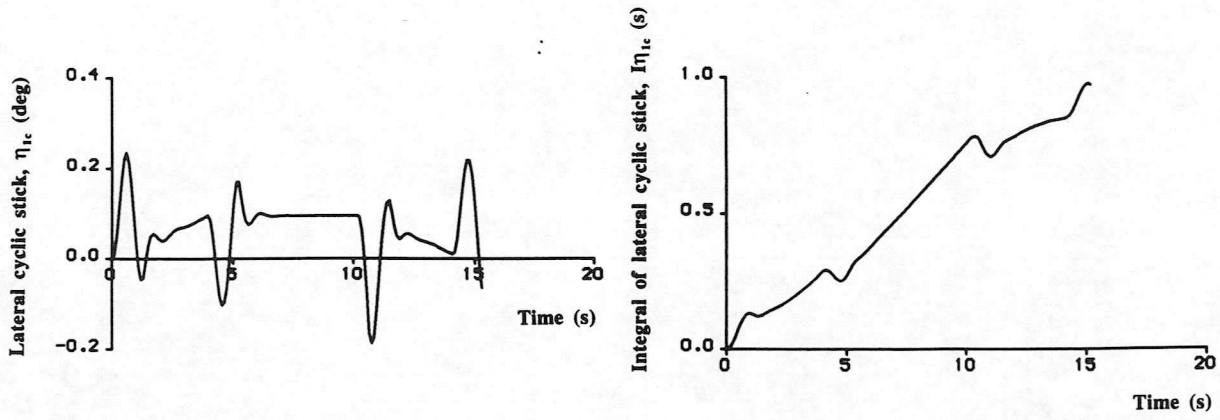

(a) Lateral cyclic actuator time constant, τ_{c2}=0.125 (normal)

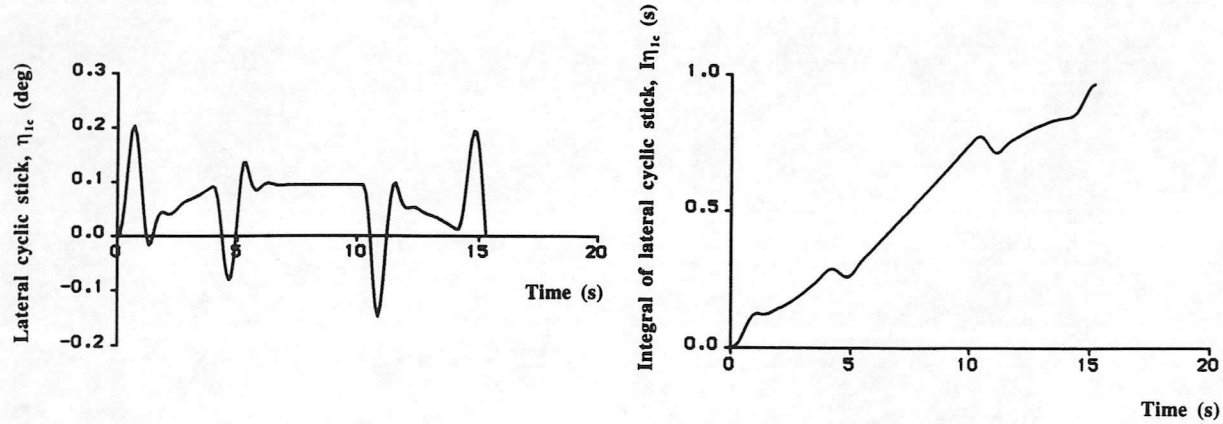

(b) Lateral cyclic actuator time constant, τ_{c2}=0.0

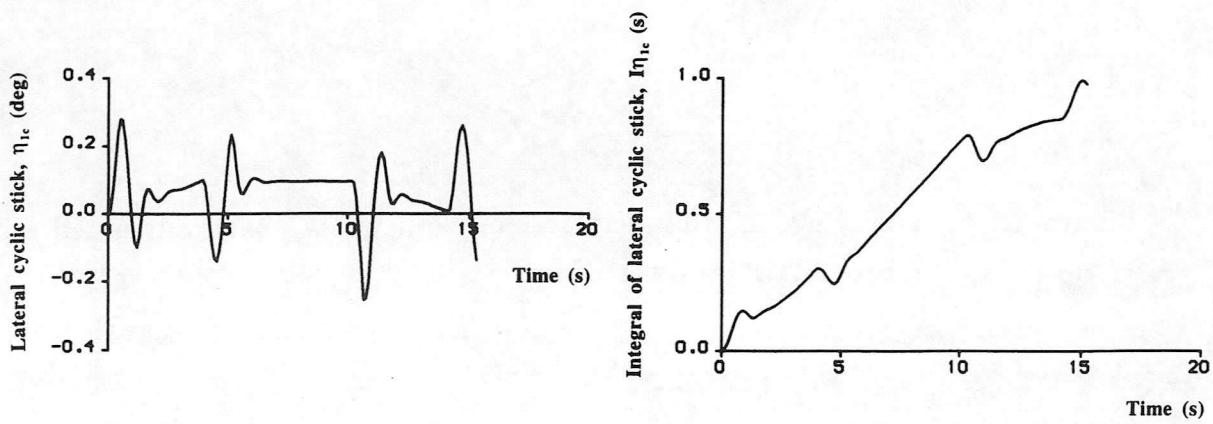

(c) Lateral cyclic actuator time constant, τ_{c2}=0.25

Figure 24 Lateral cyclic stick displacement, η_{1c} and integral of lateral cyclic stick, $I\eta_{1c}$ time-histories for Lynx-1

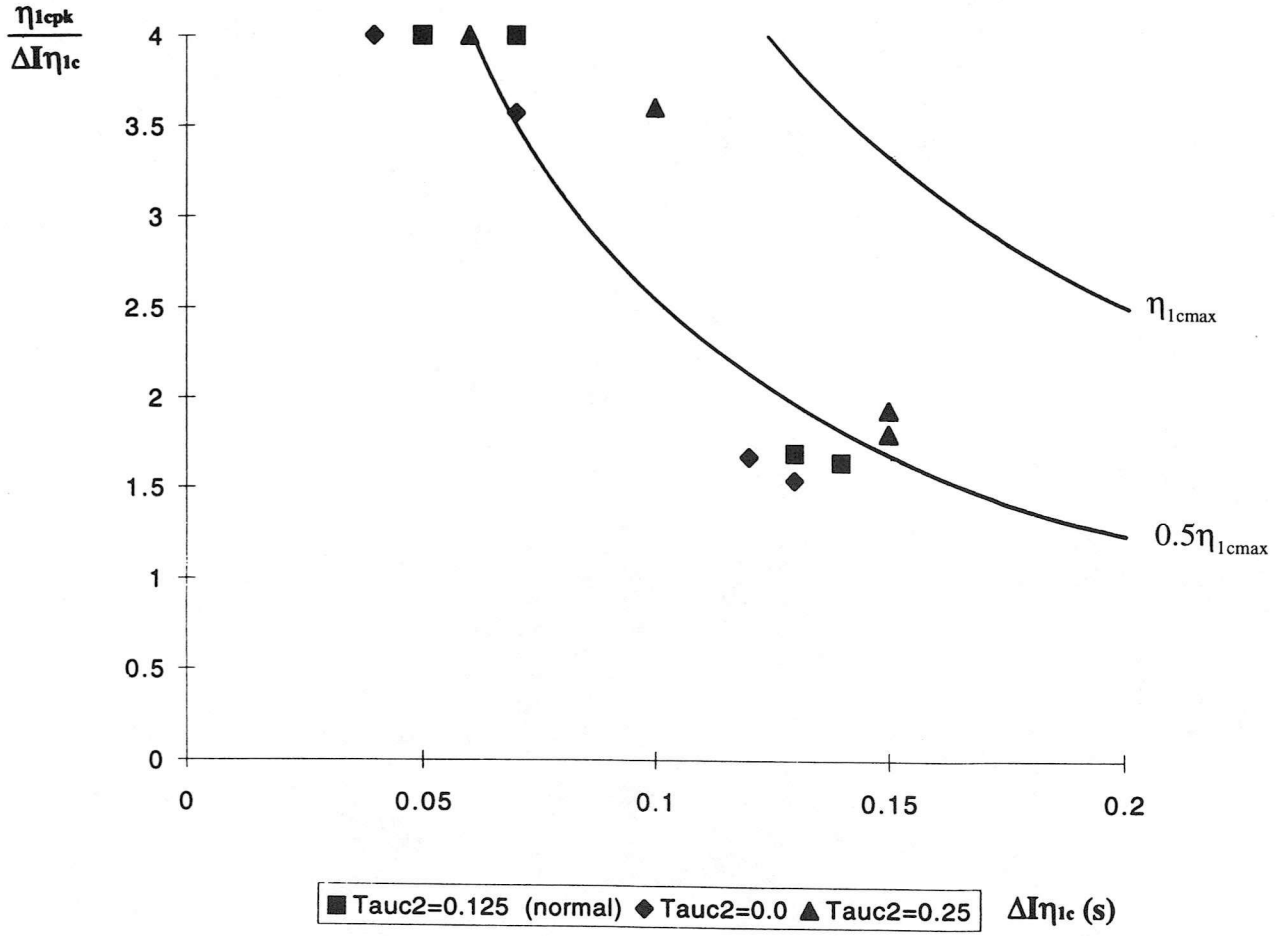

Figure 25 **Lateral cyclic stick displacement quickness chart calculated from Figure 24 time-histories**